Chapter 4

Synthesis, *In-Vitro* Antimalarial Evaluation, ADMET Properties and Molecular Docking Studies of Novel Thiazolo[3,2-*a*]pyrimidine Derivatives

4.1. Introduction

Heterocyclic molecules have received a lot of attention because of their crucial role in the new development of biologically active molecules. Approximately 70% of molecules are thought to possess heterocyclic ring systems, highlighting the significant role of heterocycles in the design and development of pharmaceutical molecules[101]. It has been revealed that number of heterocyclic compounds with a five-membered ring exhibit a variety of biological activities. Hantzsch and weber were the first authors who presented a comprehensive explanation of the formation of the thiazole ring, which has obtained significant interest from industrial and pharmaceutical researchers over the last many decades[102].

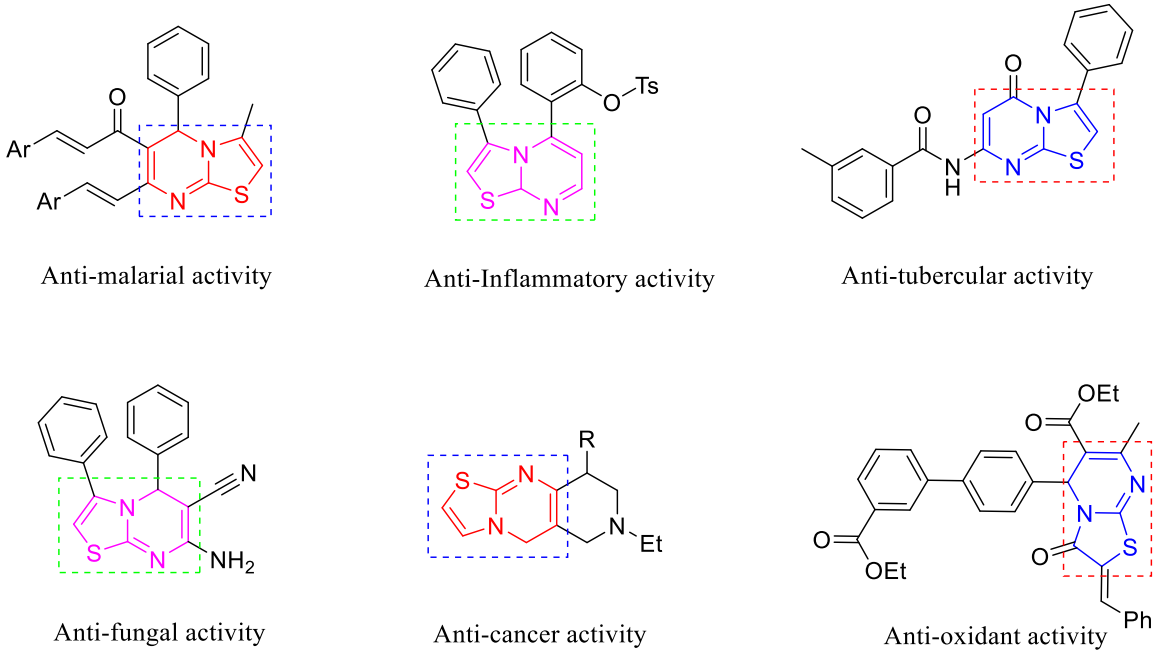

Scheme 1. Several bioactive thiazolo[3,2-*a*]pyrimidine

Thiazole found in various natural compounds, including carboxylase vitamin B, epithilone, thiamine, penicillin, and thiostrepton [103]. Thiazole derivatives have been observed to display activities such as anti-inflammatory[104], anti-viral[105], anti-microbial[106], anti-oxidant[107], anti-convulsant[108], anti-bacterial[109], anti-cancer[110], anti-fungal[111], anti-tubercular[112], anti-tumor[113], anthelmintic activity[114], anti-malarial activity[115]. The Pyrimidine ring represents a significant category of *N*-containing heterocycles that find extensive application as fundamental building blocks in the field of pharmaceuticals. It demonstrates a diverse range of biological activities, anti-bacterial[116], anti-insecticidal[117], anti-fungal[118], anti-HIV[119], anti-microbial[120], analgesic[121], anti-inflammatory[122], anti-tumor[123], anti-cancer[124] and anti-malarial agents[125]. The pyrimidine core serves as the fundamental structure in many widely recognized drugs like avanafil, etravirine, rosuvastatin, fluorouracil, iclaprim and risperidone[126]. Thiazolopyrimidines, which are fused hybrid heterocyclic molecules containing both thiazole and pyrimidine ring systems, play significant roles in pharmaceutical chemistry. It's important to highlight that thiazole and its structurally related analogs, specifically thiazolopyrimidines derivatives, form a recognized category of molecules that can serve as a foundation for developing new lead molecules. This is because of their many biological action and considerable potential for subsequent chemical modification. Thiazolopyrimidine have received a lot of interest because of their diverse array of biological activities, including, anti-hypertensive[127], anti-oxidant[128], anti-tubercular[129], anticancer [91], anti-malarial[130], anti-Parkinson's[131], anti-diabetic[132], anti-inflammatory[133], anti-histaminic[134], anti-viral[135], anti-HIV[136], anti-biofilm[137], anti-fungal[138] and anti-tumor[139]. **Scheme 1** shows numerous bioactive thiazolo[3,2-*a*]pyrimidine compounds, highlighting their potential importance in chemistry. Our ongoing efforts in the exploration of new heterocyclic molecules[140, 141] with potential pharmaceutical applications have led us to focus our efforts on the creation of new heterocyclic structures fused with a thiazole moiety as the central component. This approach aims to elevate their pharmaceutical efficacy.

4.1.1. Synthetic methods for substituted thiophene scaffold and its biological significance

Fused thiazolopyrimidine compounds were synthesized, according to H. Alzahrani[142]. This was achieved by reacting chloro thiazolopyrimidine **1** compound with dihydropyridine carbonitrile to generate thienopyridine compound **2**, which was then joined to different substituted benzaldehydes to form compound **3** in a reasonable yield. When tested against the MCF-7 cell line, the synthesized compounds exhibited good to exceptional anticancer efficacy The synthesized molecules showed good to excellent anticancer activity against MCF-7 cell line **(Scheme 4.1)**.

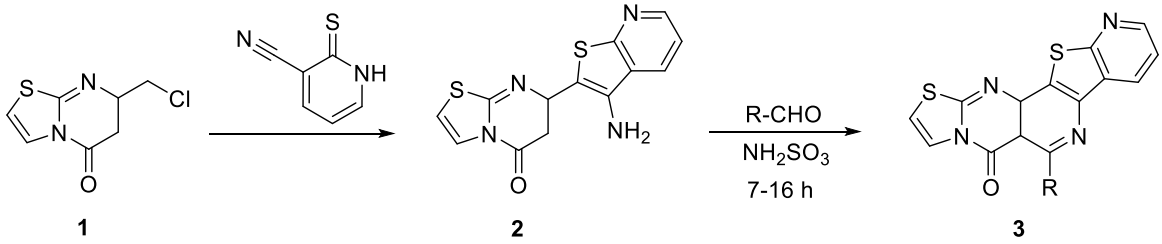

Scheme 4.1

The synthesis of novel thiazolopyrimidine compounds and their anticancer activity screening were reported by A. Mohamed[143]. The intermediate pyrido-pyrimidine compound **5** was produced by the reaction of compound **4** with amino thiazole in dimethyl sulfoxide and butanol, resulting in the fused compound **5**. The intermediate **6** was further reacted with bromo propanoic acid and chloroacetic acid in the presence of sodium acetate and refluxed in a mixture of acetic anhydride and glacial acetic acid to synthesize molecules **7** and **8 (Scheme 4.2)**. Additionally, compounds **10** and **11** were synthesized via the reaction of compound **9** with different aldehydes and diazonium salt **(Scheme 4.3)**.

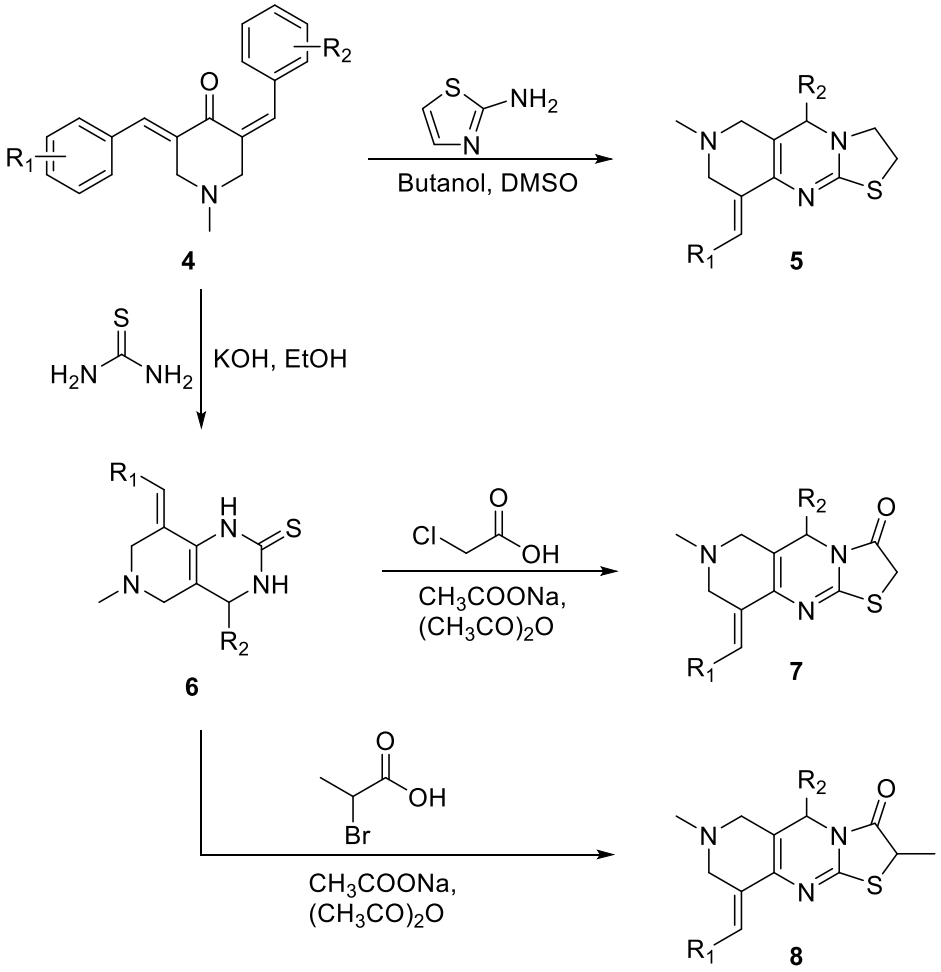

Scheme 4.2

Many of the produced compounds demonstrated exceptional inhibition against a variety of cancer cell lines when they were evaluated against a wide range of cancer cell lines.

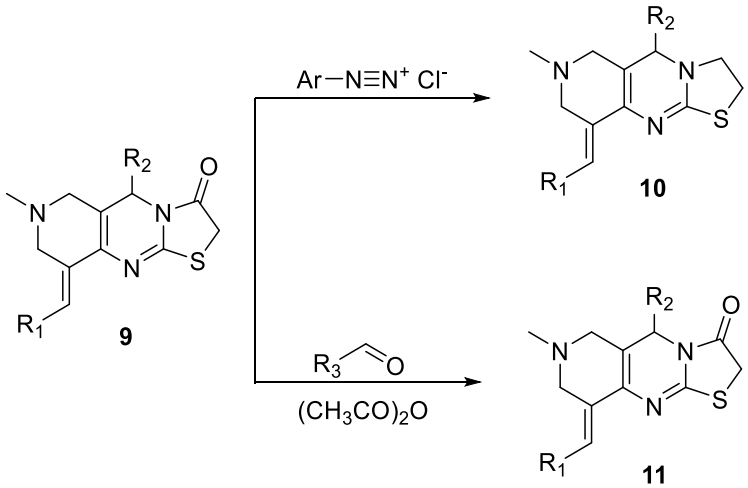

Scheme 4.3

In acetonitrile with a catalytic quantity of potassium carbonated, diethyl chloroethynyl phosphonate 1**3** reacted with tetrahydropyrimidine compound **12** to yield thiazolopyrimidine compound **14**. This innovative synthesis of phosphorylated thiazolopyrimidine compound was described by D. Egorov[144] **(Scheme 4.4)**.

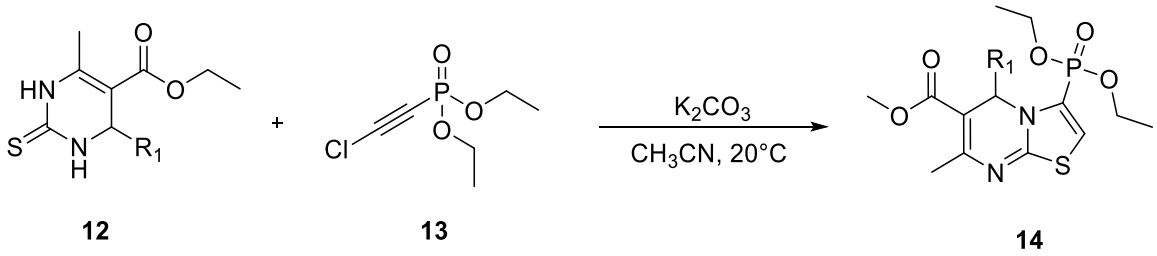

Scheme 4.4

In the research conducted by R. Aggarwal[145], a new approach for synthesizing thiazolopyrimidine compounds was explored, tetrahydropyrimidine **18** was introduced to the brominated diketone compound **17** that was created by the reaction of diketone **15** and **16** in a pestle and mortar without the use of any solvent. The mixture was then maintained in ethanol under a 27 W visible light source or heated under reflux for the proper amount of time to synthesize the fused thiazolopyrimidine compound **19** with a high yield **(Scheme 4.5)**.

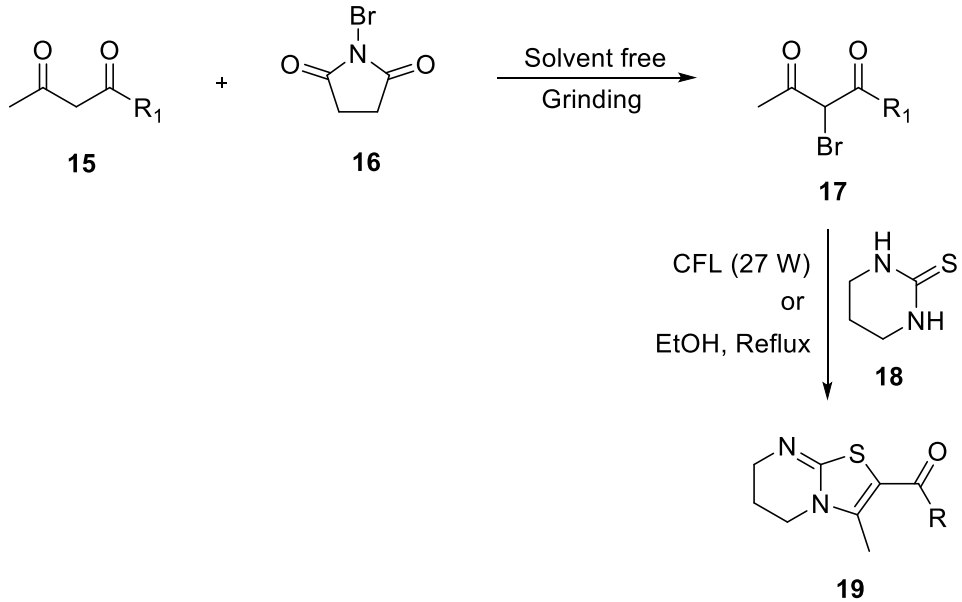

Scheme 4.5

4.2. Results and Discussion

In our investigation, we describe the identification of a unique anti-malarial component along with the synthesis of various heterocyclic molecules. We describe detailed information about 15 newly created components, each of which contains thiazolo[3,2-*a*]pyrimidine in its main structure. The compound **5a**–**o** were characterized by analyzing their spectral data, such as ^{1}H NMR, ^{13}C NMR, mass spectroscopy and FTIR. Firstly, ethyl 2-amino-4-methylthiazole-5-carboxylate **1** was produced using readily accessible reagents such as thiourea or its *N*- substituted derivative, ethyl acetoacetate and NBS[96]. Subsequently, 2-amino-4-methylthiazole-5-carbohydrazide **2** was generated through the reaction between molecule **1** and hydrazine hydrate in MeOH under reflux conditions[97]. Following this, molecules (*Z*)-2-amino-4-methyl-*N*'-(1-arylethylidene)thiazole-5-carbohydrazide **3a**–**o** were obtained by reaction of molecule **2** with different acetophenone according to our previously reported method[106]. Lastly, the reaction between molecules **3a**–**o** and 2-bis(methylthio)methylene malononitrile proceeded innovative and extensively functionalized thiazolo[3,2-*a*]pyrimidine derivatives **5a**–**o**, as show in the **Scheme 2**.

Based on their spectrum data and elemental analyses, the freshly synthesized molecules' structural assignments were determined. We provide both elemental analysis data and physical characteristics of these innovative substances. This includes presenting the NMR, mass spectroscopy and FTIR spectra of these substances. Notably, compounds exhibit a proton singlet of NH group seen between s 9.47–11.55 ppm. The aromatic region was seen between 7.03–7.77 ppm. Proton singlet of methyl group seen between 2.33–3.82 ppm. The mass spectral analysis of each compound displayed a molecular ion, confirming their molecular weights. Furthermore, the mass spectra exhibit a molecular ion peak at 426.51, corresponded to the molecular formula $C_{19}H_{18}N_6O_2S_2$.

4.2.1. Optimizing of the reaction conditions

Table 1: Optimization of the reaction conditions

Entry	Solvent	Base [a]	Temp. (C)	Time	Yield (%) [b]	Purification
1	No solvent	–	100	2h	–	–
2	H_2O	–	Rt	2h	–	–
3	H_2O	K_2CO_3	Reflux	2h	–	–
4	THF	K_2CO_3	Reflux	2h	40	Yes
5	THF	Et_3N	Reflux	2h	32	Yes
6	Acetone	K_2CO_3	Reflux	2h	41	Yes
7	Acetone	Et_3N	Reflux	2h	47	Yes
8	EtOH	K_2CO_3	Reflux	2h	38	Yes
9	EtOH	Et_3N	Reflux	2h	46	Yes
10	MeCN	K_2CO_3	Reflux	2h	42	Yes
11	MeCN	Et_3N	Reflux	2h	49	Yes
12	MeOH	K_2CO_3	Reflux	2h	68	Yes
13	MeOH	Et_3N	Reflux	2h	71	Yes
14	DMF	Et_3N	Reflux	2h	87	Yes
15	DMF	K_2CO_3	Reflux	1.5h	84	No
16	DMF	K_2CO_3	Reflux	2h	91	No
17	DMF	K_2CO_3	Reflux	2.5h	91	No

To enhance the experimental condition for the creation of novel compounds **5a**–**o**, we employed various solvent such as tetrahydrofuran, methanol, IPA, ethanol and acetone with different bases, including triethylamine and potassium carbonate. Through this study, we find that utilizing potassium carbonate together with DMF led to an accelerated reaction between (*Z*)-2-amino-4-methyl-*N*'-(1-arylethylidene)thiazole-5-carbohydrazide **3a**–**o** and 2-bis(methylthio)methylene malononitrile 4, as a result of a more rapid process and a favorable yield of thiazole derivative (*Z*)-*N*'-(1-(aryl)ethylidene)-6-cyano-5-imino-3-methyl-7-(methylthio)-5*H*-thiazolo[3,2-*a*]pyrimidine-2-carbohydrazide **5a**–**o**.

The initial reaction was conducted at 100°C without employing any catalyst or base, yielding no results (**Table 1**, entry 1). Subsequently, we attempted the reaction utilizing water as a solvent and without a base at ambient temperature, but no product formation occurred (entry 2). In an effort to improve the process, we introduced potassium carbonate and refluxed the mixture for 2 hour. However, this didn't result in the desired product

formation (entry 3). Shifting our approach, we utilized potassium carbonate as a base and conducted the reaction in tetrahydrofuran under reflux for 2 hour, resulting in a 40% product yield (entry 4). Similarly, using triethylamine as the base in tetrahydrofuran provided a 32% product yield (entry 5). Subsequently, we adjusted the reaction conditions by changing the solvent to acetone and employing potassium carbonate as the base. This led to a product yield of 41% (entry 6), whereas using triethylamine as the base increased the yield to 47% (entry 7). Further refinement was achieved by switching to ethanol as the solvent and utilizing potassium carbonate as the base. Refluxing the mixture for 2 hour resulted in a 38% yield (entry 8), which enhanced to 46% when triethylamine was utilized as a base (entry 9). Exploring alternative conditions, we utilized acetonitrile as the solvent and potassium carbonate as the base, producing a 42% product yield (entry 10). Similarly, employing triethylamine as a base at those conditions resulted in a 49% yield (entry 11). Interestingly, when employing methanol as the solvent and potassium carbonate as the base, the yield increased to 68% (entry 12). This enhancement was substantially more significant when using triethylamine as the base, achieving a yield of 71% (entry 13). Notably, the utilization of *N*, *N*-dimethylformamide with triethylamine yielded an 87% yield (entry 14). It can be concluded that the duration of reflux has a significant impact on the yield of the reaction when potassium carbonate is used as the base. Specifically, a reflux time of 1.5 hours results in a lower yield of 84% (entry 15), indicating that this duration is insufficient for maximizing the reaction's efficiency. However, extending the reflux time to 2 hours substantially improves the yield to 91% (entry 16), demonstrating that this duration is more optimal for the reaction conditions. Interestingly, further increasing the reflux time to 2.5 hours does not lead to any improvement in the yield, as it remains at 91% (entry 17). This suggests that prolonging the reflux beyond 2 hours does not contribute to further enhancements in yield. Therefore, for this reaction system, refluxing for 2 hours is the most effective duration, balancing time and efficiency, as it achieves the highest observed yield without any additional benefits from longer reflux times. Our approach was used to develop novel thiazolo[3,2-*a*]pyrimidine compounds, as shown in **Table 2**.

Scheme 2. Reagents and conditions.

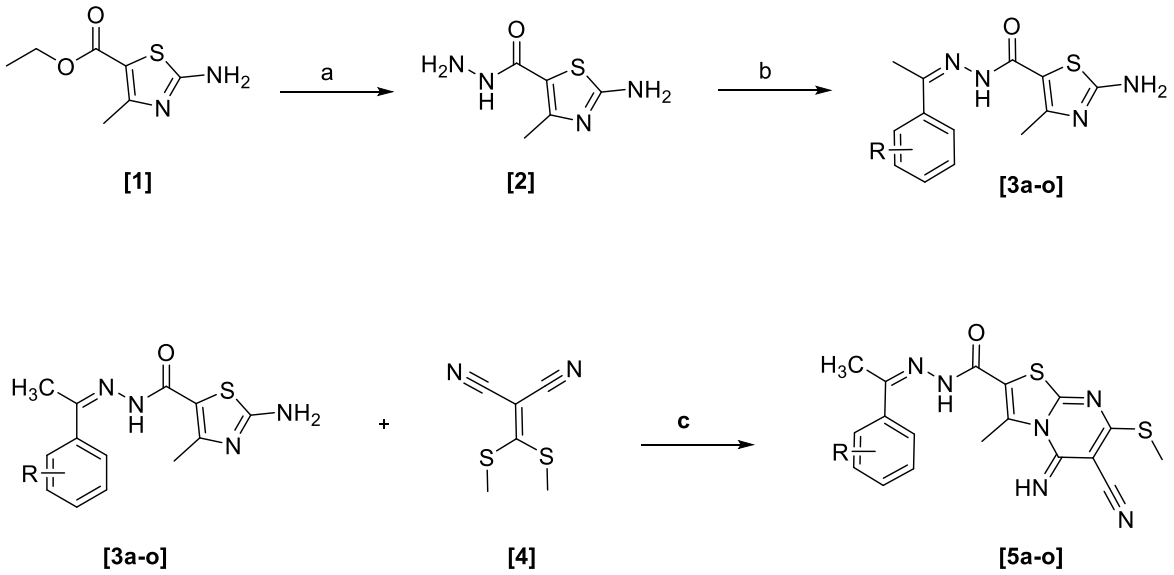

(a) $NH_2NH_2.H_2O$, MeOH, reflux, 1h (b) Substituted acetophenone, CH_3COOH, MeOH, reflux, 1h (c) K_2CO_3, DMF, reflux, 2h.

4.2.2. Physicochemical characteristeristics

Table 2: Physicochemical characteristics of novel thiazolo[3,2-*a*]pyrimidine derivatives 5a–o

Entry	R	Molecular Formula	Molecular Weight	Melting Point (°C)	Yield (%)[a]	
					5a-o	4a-o
5a	4-OCH_3	$C_{19}H_{18}N_6O_2S_2$	426.51	205–207	89	85
5b	4-Cl	$C_{18}H_{15}ClN_6OS_2$	430.93	232–234	81	87
5c	4-CH_3	$C_{19}H_{18}N_6OS_2$	410.51	209–211	88	91
5d	4-Br	$C_{18}H_{15}BrN_6OS_2$	475.38	242–244	82	86
5e	2-OCH_3, 4-F	$C_{19}H_{17}FN_6O_2S_2$	444.50	227–229	87	82
5f	2,4-Cl	$C_{18}H_{14}Cl_2N_6OS_2$	465.37	224–226	83	81
5g	4-F	$C_{18}H_{15}FN_6OS_2$	414.48	215–217	84	89
5h	H	$C_{18}H_{16}N_6OS_2$	396.49	202–204	86	82
5i	2-Cl, 5-Br	$C_{18}H_{14}BrClN_6OS_2$	509.83	248–250	85	88
5j	4-NO_2	$C_{18}H_{15}N_7O_3S_2$	441.48	217–219	80	84

5k	2-OH, 4-F	$C_{18}H_{15}FN_6O_2S_2$	430.48	223–225	82	78
5l	2-CH_3	$C_{19}H_{18}N_6OS_2$	410.51	213–215	87	80
5m	4-OH	$C_{18}H_{16}N_6O_2S_2$	412.49	210–212	84	77
5n	2-OH	$C_{18}H_{16}N_6O_2S_2$	412.49	204–206	75	76
5o	3-OH	$C_{18}H_{16}N_6O_2S_2$	412.49	201–203	71	79

4.2.3. *In vitro* antimalarial screening

We assessed the anti-malarial evaluation of the recently synthesized hybrid molecules **5a–o** against a Plasmodium falciparum. The results of the experimental protocols are illustrated in **Table 3**. The result of experimental protocol's revealed that the tested molecules showed moderate to good levels of inhibition.

Table 3. Antimalarial activity

Entry	**IC_{50} (µg/ml)**
5a	0.19 ± 0.002
5b	0.093 ± 0.003
5c	0.25 ± 0.002
5d	0.11 ± 0.005
5e	0.22 ± 0.001
5f	0.098 ± 0.004
5g	0.16 ± 0.002
5h	0.34 ± 0.001
5i	0.13 ± 0.005
5j	0.39 ± 0.003
5k	0.24 ± 0.001
5l	0.31 ± 0.002
5m	0.28 ± 0.005
5n	0.36 ± 0.004
5o	0.37 ± 0.003
Chloroquine	0.023 ± 0.001

It was discovered that among the molecules **5a**–**o**, molecule **5b** and **5f** showed the most substantial activity because of attachment of chloro group. Molecule **5b** with IC_{50} value of 0.093 ± 0.003 and Molecule **5f** with IC_{50} value of 0.098 ± 0.004. Molecule **5a** having methoxy substitution on *para* position showed moderate activity against Plasmodium falciparum. Molecule **5c** having methyl substitution demonstrated moderate action against Plasmodium falciparum. Molecule **5d**, molecule **5e**, molecule **5g** and molecule **5i** showed good activity due to attachment of halogen group. Molecule **5h** showed moderate activity.

Molecule **5j** having nitro group on para position indicated moderate activity. Molecule **5k** showed good activity. Molecule **5l** having methyl group indicated moderate activity. Molecule **5m**, **5n** and **5o** having a hydroxy substitution on ortho, meta and para position indicated moderate activity.

4.2.4. Molecular Docking

We conduct a molecular docking analysis on PfDHFR enzyme using Autodock vina 1.5.7 to identify binding sites of potent compound. The crystal structure of PfDHFR enzyme with PDB id 3QGT was obtained from the Protein Data Bank. The validation of the docking study was carried out by redocking and superimposing the co-crystallized ligand with the ligand extracted from the crystal structure. The root mean square deviation (RMSD) was determined to be 0.068 Ångstrom, demonstrating the accuracy and reliability of the molecular docking procedure (Figure 1). Significantly active component **5b** formed conventional hydrogen bonds with TYR A:170 achieving a docking score of –9.0 (Figure 2). While significantly active component 5f formed conventional hydrogen bonds with TYR A:170 achieving a docking score of –9.3 (Figure 3). The docking scores of significantly active molecule **5b** and **5f** batter than standard drug chloroquine which show docking score of –7.5.

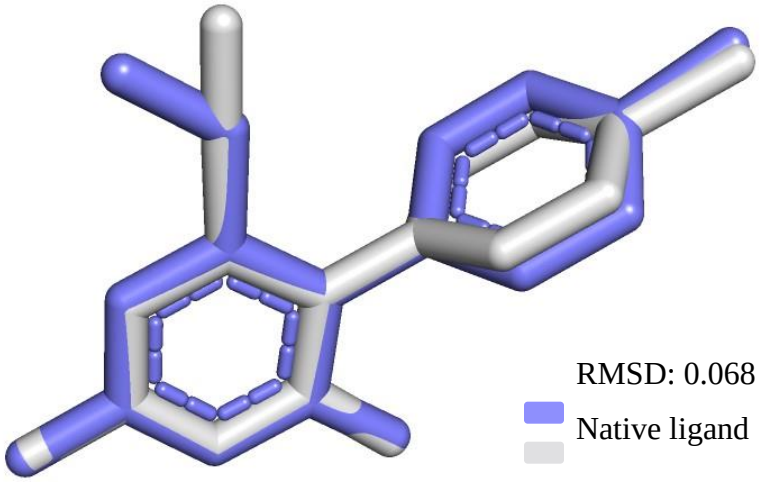

Fig 1. Validation of molecular docking protocol.

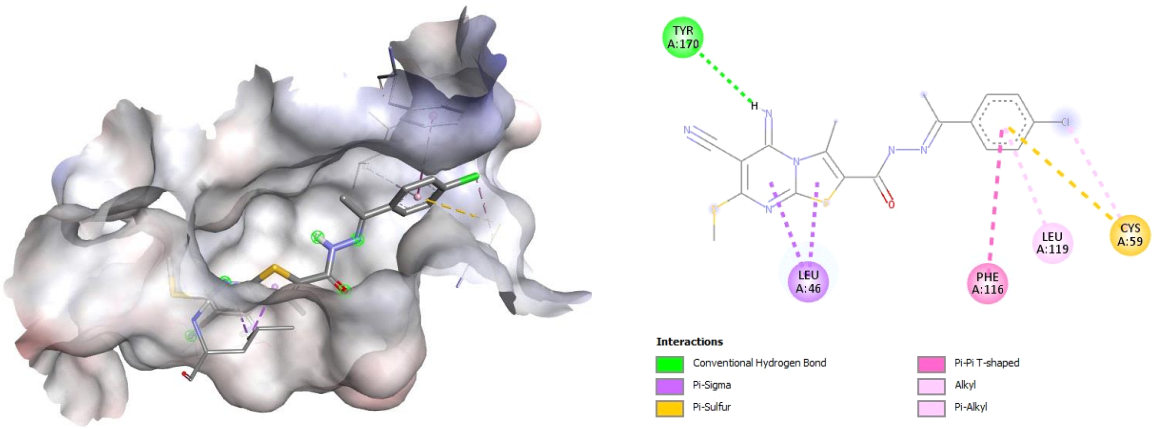

Fig 2. 2D and 3D binding interactions of compound 5b

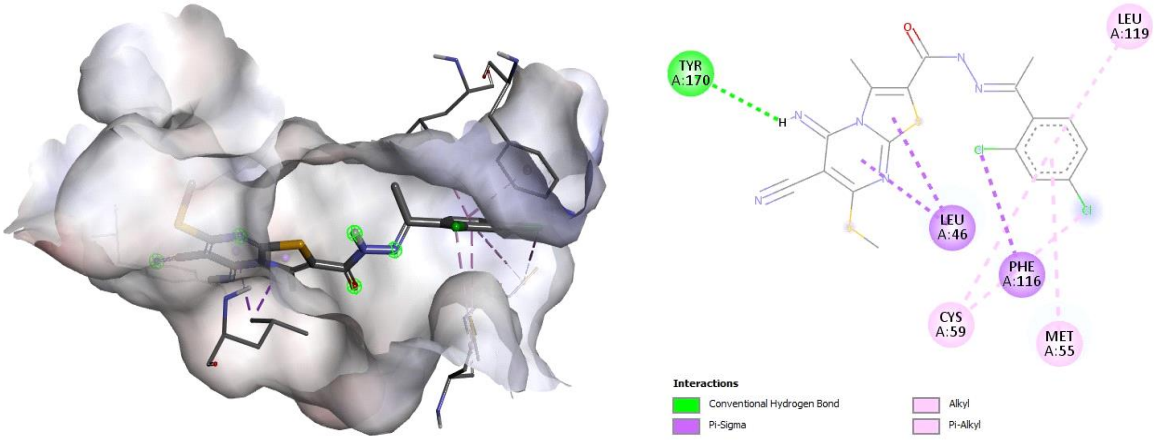

Fig 3. 2D and 3D binding interactions of compound 5f

4.2.5. Prediction of the ADMET properties

In the drug discovery process many potential drug candidates face failure because of their inadequate pharmacokinetics and physicochemical properties. These limitations can be effectively addressed during the initial investigation phase by utilizing computational ADMET methods to analyze novel synthesized compounds. The newly synthesized Thiazolo[3,2-*a*]pyrimidine molecules' ADMET parameters such as Lipinski's Rule of five (RoF (V)), Synthetic Accessibility (SA), skin permeation (Log K_p), gastrointestinal absorption (GIA), Lipophilicity (Log $P_{o/w}$), Topological polar surface area (TSPA), Water Solubility (Log S), H-bond donor (HBD) and H-bond acceptor (HBA) are displayed in **Table 4**. Almost all synthetic molecules bioavailability could be predicted based on their water solubility (Log S), the results revealed that all thiazole[3,2-a] derivatives scored between –5.64 and –7.01 and Lipophilicity (Log Po/w) lower than 5 (in the range of 2.09 to 3.89). Almost all synthetic molecules adhere to Lipinski's Rule of five, with the exception of 5i, which having a higher molecular weight than 500. Additionally, the synthetic accessibility test was used to evaluate the complexity of newly synthesized compound's molecular structures. The results revealed that all thiazole derivatives scored between 3.48 and 3.63. Utilizing Swiss ADME, the computational data are processed[98].

Table 4. Physicochemical, Pharmacokinetic and Medicinal Chemistry Properties of the synthesized Molecule 5a–o

Physicochemical properties						**Pharmacokinetics**		**Medicinal chemistry**	
Compound	**HBA**	**HBD**	**TSPA**	**Log $P_{o/w}$**	**Log S**	**GIA**	**Log K_p**	**RoF (V)**	**SA**
5a	6	2	169.17	2.82	–5.80	Low	–7.06	Yes	3.59
5b	5	2	159.94	3.29	–6.29	Low	–6.61	Yes	3.49
5c	5	2	159.94	3.05	–6.01	Low	–6.68	Yes	3.60
5d	5	2	159.94	3.38	–6.36	Low	–6.84	Yes	3.51
5e	7	2	169.17	3.05	–5.91	Low	–7.09	Yes	3.63
5f	5	2	159.94	3.78	–6.95	Low	–6.38	Yes	3.54
5g	6	2	159.94	3.04	–5.74	Low	–6.89	Yes	3.48
5h	5	2	159.94	2.72	–5.64	Low	–6.85	Yes	3.50
5i	5	2	159.94	3.89	–7.01	Low	–6.61	No	3.55
5j	7	2	205.76	2.09	–6.42	Low	–7.25	Yes	3.56
5k	7	3	180.17	2.58	–5.80	Low	–7.24	Yes	3.53
5l	5	2	159.94	3.08	–6.01	Low	–6.68	Yes	3.61
5m	6	3	180.17	2.32	–5.69	Low	–7.2	Yes	3.51

5n	6	3	180.17	2.34	–5.69	Low	–7.2	Yes	3.54
5o	6	3	180.17	2.29	–5.69	Low	–7.2	Yes	3.51
Chloroquine	2	1	28.16	4.15	-4.95	High	-4.96	Yes	2.76

HBA H-bond acceptor, *HBD* H-bond donor, *TPSA* topologic polar surface area, *Log* $P_{o/w}$ lipophilicity, *Log S* water solubility, *GIA* gastrointestinal absorption, *Log* K_p skin permeation, *RoF (V)* Lipinski's rule of five,*SA* synthetic accessibility

4.3. Conclusion

In the present research study, a series of novel (*Z*)-*N*'-(1-(aryl)ethylidene)-6-cyano-5-imino-3-methyl-7-(methylthio)-5*H*-thiazolo[3,2-*a*]pyrimidine-2-carbohydrazide **5a**–**o** have been synthesized. The newly synthesized molecule has been validated by ^{1}H NMR, ^{13}C NMR, FTIR and mass spectroscopic analysis. All the synthesized compounds were evaluated for their antimalarial activity. Docking study of significantly active compound was performed. An analysis of their physicochemical and pharmacokinetic properties related to ADMET has been also carried out.

4.4. Experimental Section

An electro thermal device paired with an open capillary was employed to determine melting points, and these values remained unaltered without any adjustments. silica-gel 60 F254 precoated plates from Merck were utilized for thin-layer chromatography. Molecule visualization was accomplished using either UV light at 365 nm and 264 nm or with iodine vapor. For the recording of IR spectra, the ATR technique was put into practice using a Shimadzu FT-IR spectrometer. When acquiring ^{1}H spectra, a Bruker AVANCE III (400 MHz) spectrometer was employed under DMSO-d_6 conditions. Chemical shifts are denoted in δ ppm relative to Tetramethylsilane (TMS), which was used as the internal standard. To obtain mass spectra, a direct inlet probe was utilized together with a Shimadzu GCMS QP2010 Ultra mass spectrometer. All required reagents were purchased from sources labeled as Sigma-Aldrich, SRL, Avra, CDH, TCI, Loba, Apollo, SDFCL, Combi-Blocks BLD pharm and Spectrochem, and they used without further purification.

- **General Methodology for synthesis of 2-amino-4-methylthiazole-5-carbohydrazide (2).**

Molecule **1** (40 mmol) was dissolved in 40 ml of EtOH, and then hydrazine hydrate (80 mmol) was introduced to the solution, followed by refluxing for a duration of 14 hours. Once the reaction had completed, the resulting mixture was cooled, and the solid that emerged in the beaker was subjected to filtration. The obtained filtrate was subsequently recrystallized from ethanol, resulting in the isolation of the pure product. Yield 72%.

- **General Methodology for synthesis of (*Z*)-2-amino-4-methyl-*N*'-(1-arylethylidene)thiazole-5-carbohydrazide (3a–o).**

A mixture of molecule **2** (40 mmol) and a substituted acetophenone (40 mmol) was combined with 40 ml of methanol, and a catalytic amount of glacial acetic acid was used as a catalyst. The mixture was heated to a high temperature and kept at that temperature for 1 h. After the reaction is finished, the mixture was allowed to cool to room temperature and poured into water. After that neutralized the reaction mixture with dil. HCl. The solid product was separated by filtering, and it was then washed with a water. To make the product purer, it underwent a process where it was dissolved in ethanol and then allowed

to crystallize again. This resulted in obtaining the final pure product **(3a–o)**.

- **General Methodology for synthesis of (*Z*)-6-cyano-5-imino-3-methyl-7-(methylthio)-*N*'-(1-phenylethylidene)-5*H*-thiazolo[3,2-*a*]pyrimidine-2-carbohydrazide (5a–o).**

A mixture containing molecule **3a–o** (20 mmol) and 2-bis(methylthio)methylene malononitrile **4** (20 mmol) was combined with 20 ml of DMF, and anhydrous K_2CO_3 (20 mmol) was added as catalyst. After that, mixture was heated to reflux temperature for 2 hour. Once the reaction is completed, the suspension was cool down to ambient temperature then mixture was added to the crushed ice. Reaction mixture was neutralized with dilute HCl. The resulting solid was separated and filtered, followed by a washing process using a water. The acquired final product was then purified through recrystallization from DMF. This resulted in obtaining the final pure yellow color compounds **5a–o.**

(*Z*)-6-cyano-5-imino-*N*'-(1-(4-methoxyphenyl)ethylidene)-3-methyl-7-(methylthio)-5*H*-thiazolo[3,2-a]pyrimidine-2-carbohydrazide (5a).

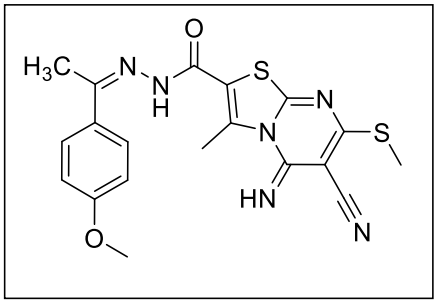

Yield 89%, mp 205–207 °C. IR spectrum, *ν*, cm^{-1}: 1651.12 (C=O), 2205.78 (CN), 2939.61 (CH_3), 3286.81 (-NH). ^1H NMR spectrum, *δ*, ppm: 2.34 s (3H, CH3), 2.54 s (3H, CH_3), 2.90 s (3H, CH_3), 3.82 s (3H, CH_3), 7.03 d (2H, *J* = 8 Hz, C_6H_4), 7.75 d (2H, *J* = 6.8 Hz, C_6H_4), 11.29 s (1H, NH). Found, %: C 53.54; H 4.22; N 19.73. $C_{19}H_{18}N_6O_2S_2$. Calculated, %: C 53.51; H, 4.25; N, 19.70. *M* 426.

(*Z*)-*N*'-(1-(4-chlorophenyl)ethylidene)-6-cyano-5-imino-3-methyl-7-(methylthio)-5*H*-thiazolo[3,2-*a*]pyrimidine-2-carbohydrazide (5b).

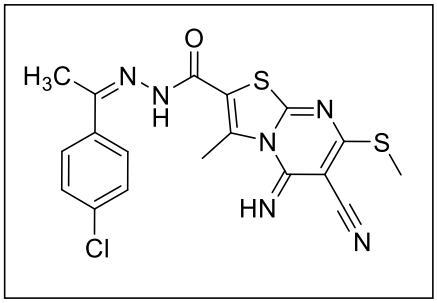

Yield 81%, mp 232–234 °C. IR spectrum, *v*, cm^{-1}: 1667.84 (C=O), 2205.11 (CN), 2927.20 (CH_3), 3305.71 (-NH). ^1H NMR spectrum, *δ*, ppm: 2.34 s (3H, CH_3), 2.55 s (3H, CH_3), 2.90 s (3H, CH_3), 7.45 d (2H, *J* = 8.8 Hz, C_6H_4), 7.69 d (2H, *J* = 8.8 Hz, C_6H_4), 11.29 s (1H, NH). Found, %: C 50.19, H 3.54, N 19.52. $C_{18}H_{15}ClN_6OS_2$. Calculated, %: C, 50.17; H, 3.51; N, 19.50. *M* 430.

(*Z*)-6-cyano-5-imino-3-methyl-7-(methylthio)-*N*'-(1-(p-tolyl)ethylidene)-5*H*-thiazolo[3,2-*a*]pyrimidine-2-carbohydrazide (5c).

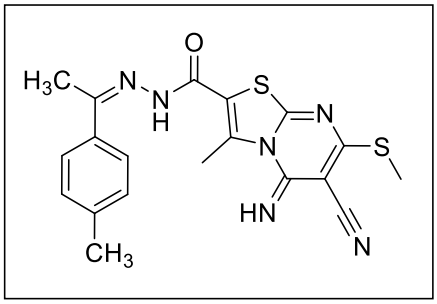

Yield 88%, mp 209–211 °C. IR spectrum, *v*, cm^{-1}: 1651.12 (C=O), 2202.78 (CN), 2924.18 (CH_3), 3282.95 (-NH). ^1H NMR spectrum, *δ*, ppm: 2.37 s (3H, CH_3), 2.53 s (3H, CH_3), 2.54 s (3H, CH_3), 2.93 s (3H, CH_3), 7.30 d (2H, *J* = 18.4 Hz, C_6H_4), 7.72 d (2H, *J* = 12.8 Hz, C_6H_4), 9.48 s (1H, NH), 11.34 s (1H, NH). ^{13}C NMR spectrum, *δ*, ppm: 13.6 (C-16), 16.4 (C-15), 21.1 (C-28), 26.6 (C-21), 84.0 (C-4), 112.1 (C-9), 117.8 (C-18), 128.2 (C-23, C-27), 129.2 (C-24, C-26), 134.3 (C-22), 140.2 (C-25), 143.6 (C-20), 154.0 (C-1), 158.3 (C-5), 160.0 (C-8), 164.1 (C-3), 173.6 (C-10). Found, %: C 55.56, H 4.45, N 20.46%. $C_{19}H_{18}N_6OS_2$. Calculated, %: C, 55.59; H, 4.42; N, 20.47. *M* 410.

(*Z*)-*N*'-(1-(4-bromophenyl)ethylidene)-6-cyano-5-imino-3-methyl-7-(methylthio)-5*H*-thiazolo[3,2-*a*]pyrimidine-2-carbohydrazide (5d).

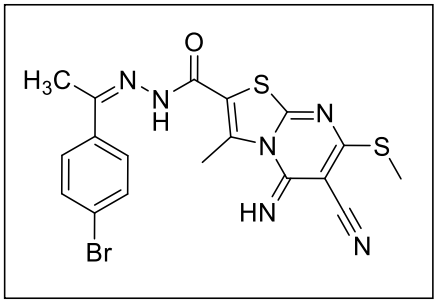

Yield 82%, mp 242–24 °C. IR spectrum, *v*, cm^{-1}: 1659.21 (C=O), 2207.25 (CN), 2930.65 (CH_3), 3292.41 (-NH). ^1H NMR spectrum, *δ*, ppm: 2.35 s (3H, CH_3), 2.54 s (3H, CH_3), 2.89 s (3H, CH_3), 7.71 dd (4H, *J* = 8.4 Hz, C_6H_4), 11.42 s (1H, NH). ^{13}C NMR spectrum, *δ*, ppm: 13.6 (C-16), 16.4 (C-15), 26.7 (C-21), 84.0 (C-4), 112.1 (C-9), 117.9 (C-18), 127.2 (C-25), 130.2 (C-23, C-27), 131.7 (C-24, C-26), 135.6 (C-22), 140.2 (C-20), 154.0 (C-1), 158.3 (C-5), 160.1 (C-8), 164.1 (C-3), 173.6 (C-10). Found, %: C 45.50, H 3.15, N 17.71. $C_{18}H_{15}BrN_6OS_2$, Calculated, %: C, 45.48; H, 3.18; N, 17.68. *M* 475.

(*Z*)-6-cyano-*N*'-(1-(4-fluoro-2-methoxyphenyl)ethylidene)-5-imino-3-methyl-7-(methylthio)-5*H*-thiazolo[3,2-*a*]pyrimidine-2-carbohydrazide (5e).

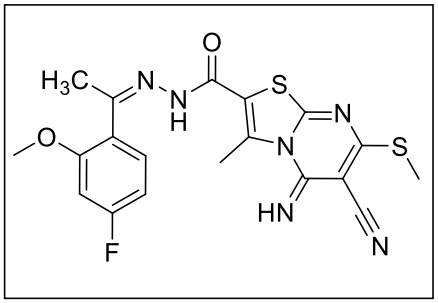

Yield: 87%, mp 227–229 °C. IR spectrum, *v*, cm^{-1}: 1662.69 (C=O), 2202.78 (CN), 2939.61 (CH_3). Found, %: C 51.36, H 3.89, N 18.94. $C_{19}H_{17}FN_6O_2S_2$. Calculated, %: C, 51.34; H, 3.86; N, 18.91. *M* 444.

(*Z*)-6-cyano-*N*'-(1-(2,4-dichlorophenyl)ethylidene)-5-imino-3-methyl-7-(methylthio)-5*H*-thiazolo[3,2-*a*]pyrimidine-2-carbohydrazide (5f).

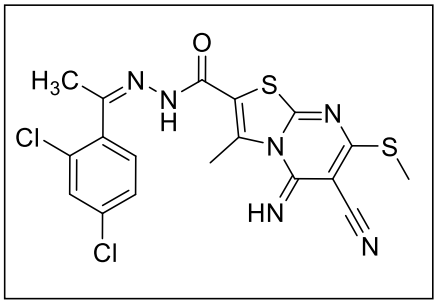

Yield 83%, mp 224–226 °C. IR spectrum, *v*, cm^{-1}: 1666.65 (C=O), 2202.78 (CN), 2924.18 (CH_3), 3302.24 (-NH). ^1H NMR spectrum, *δ*, ppm: 2.32 s (3H, CH_3), 2.54 s (3H, CH_3), 2.92 s (3H, CH_3), 7.58 d (2H, C_6H_4), 7.77 s (2H, C_6H_4), 9.49 s (1H, NH), 11.54 s (1H, NH). Found, %: C 46.43, H 3.06, N 18.09. $C_{18}H_{14}Cl_2N_6OS_2$. Calculated, %: C, 46.46; H, 3.03; N, 18.06. M 465.

(*Z*)-6-cyano-*N*'-(1-(4-fluorophenyl)ethylidene)-5-imino-3-methyl-7-(methylthio)-5*H*-thiazolo[3,2-*a*]pyrimidine-2-carbohydrazide (5g).

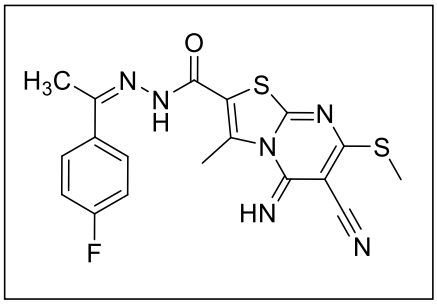

Yield 84%, mp 215–217 °C. IR spectrum, *v*, cm^{-1}: 1658.84 (C=O), 2206.64 (CN), 2928.04 (CH_3), 3290.67 (-NH). Found, %: C 52.19, H 3.67, N 20.31. $C_{18}H_{15}FN_6OS_2$. Calculated, %: C, 52.16; H, 3.65; N, 20.28. *M* 414.

(*Z*)-6-cyano-5-imino-3-methyl-7-(methylthio)-*N*'-(1-phenylethylidene)-5*H*-thiazolo[3,2-*a*]pyrimidine-2-carbohydrazide (5h).

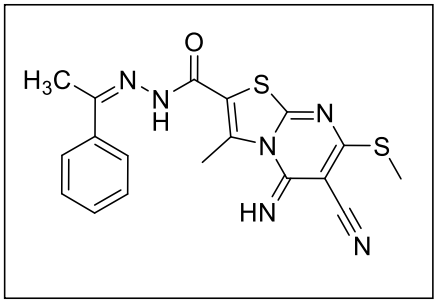

Yield 86%, mp 202–204 °C. IR spectrum, *v*, cm^{-1}: 1651.12 (C=O), 2206.64 (CN), 2931.90 (CH_3), 3275.24 (-NH). Found, %: C 54.51, H 4.09, N 21.23. $C_{18}H_{16}N_6OS_2$. Calculated, %: C, 54.53; H, 4.07; N, 21.20. *M* 396.

(*Z*)-*N*'-(1-(5-bromo-2-chlorophenyl)ethylidene)-6-cyano-5-imino-3-methyl-7-(methylthio)-5*H*-thiazolo[3,2-*a*]pyrimidine-2-carbohydrazide (5i).

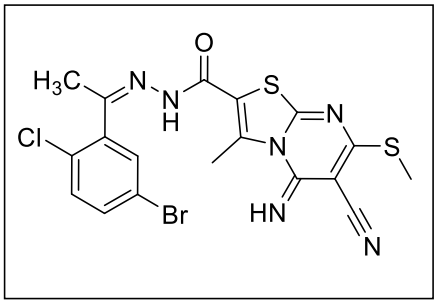

Yield 85%, mp 248–250 °C. IR spectrum, *v*, cm^{-1}: 1665.21 (C=O), 2201.91 (CN), 2922.74 (CH_3), 3301.17 (-NH). Found, %: C 42.38, H 2.75, N 16.51. $C_{18}H_{14}BrClN_6OS$. Calculated, %: C, 42.41; H, 2.77; N, 16.48. *M* 509.

(*Z*)-6-cyano-5-imino-3-methyl-7-(methylthio)-*N*'-(1-(4-nitrophenyl)ethylidene)-5*H*-thiazolo[3,2-*a*]pyrimidine-2-carbohydrazide (5j).

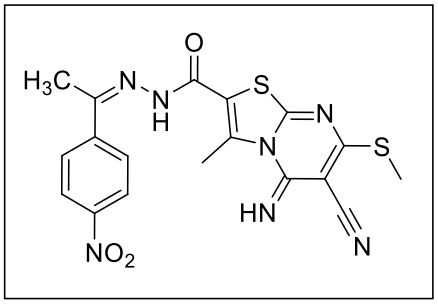

Yield 80%, mp 217–219 °C. IR spectrum, *v*, cm^{-1}: 1655.34 (C=O), 2205.34 (CN), 2925.65 (CH_3), 3289.22 (-NH). Found, %: C 48.99, H 3.39, N 22.18. $C_{18}H_{15}N_7O_3S_2$. Calculated, %: C, 48.97; H, 3.42; N, 22.21. *M* 441.

(*Z*)-6-cyano-*N*'-(1-(4-fluoro-2-hydroxyphenyl)ethylidene)-5-imino-3-methyl-7-(methylthio)-5*H*-thiazolo[3,2-*a*]pyrimidine-2-carbohydrazide (5k).

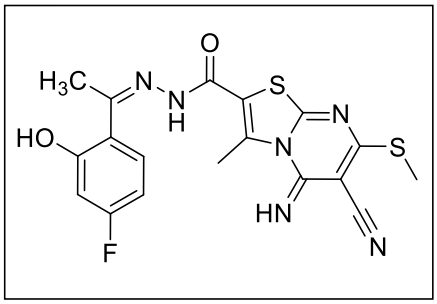

Yield 82%, mp 223–225 °C. IR spectrum, *v*, cm^{-1}: 1665.41 (C=O), 2203.11 (CN), 2939.36 (CH_3). Found, %: C 50.25, H 3.54, N 19.54. $C_{18}H_{15}FN_6O_2S_2$. Calculated, %: C, 50.22; H, 3.51; N, 19.52. *M* 430.

(*Z*)-6-cyano-5-imino-3-methyl-7-(methylthio)-*N*'-(1-(o-tolyl)ethylidene)-5*H*-thiazolo[3,2-*a*]pyrimidine-2-carbohydrazide (5l).

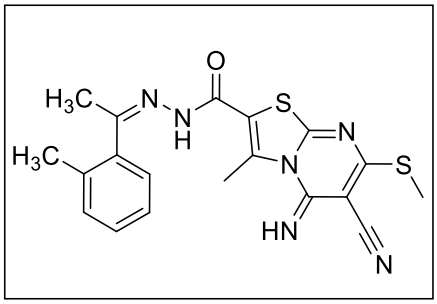

Yield 87%, mp 213–215 °C. IR spectrum, *v*, cm^{-1}: 1650.27 (C=O), 2205.11 (CN), 2928.18 (CH_3), 3272.36 (-NH). Found, %: C 55.57, H 4.39, N 20.49. $C_{19}H_{18}N_6OS_2$. Calculated, %: C, 55.59; H, 4.42; N, 20.47. *M* 410.

(*Z*)-6-cyano-*N*'-(1-(4-hydroxyphenyl)ethylidene)-5-imino-3-methyl-7-(methylthio)-5*H*-thiazolo[3,2-*a*]pyrimidine-2-carbohydrazide (5m).

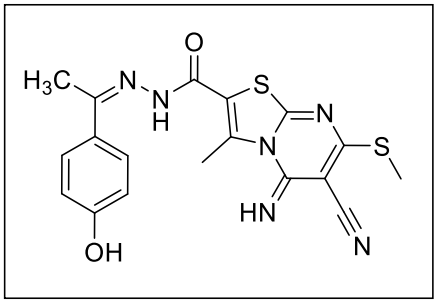

Yield 84%, mp 210–212 °C. IR spectrum, *v*, cm^{-1}: 1652.36 (C=O), 2203.10 (CN), 2940.21 (CH_3), 3287.30 (-NH). Found, %: C 52.43, H 3.88, N 20.40. $C_{18}H_{16}N_6O_2S_2$. Calculated, %: C, 52.41; H, 3.91; N, 20.37. *M* 412.

(*Z*)-6-cyano-*N*'-(1-(2-hydroxyphenyl)ethylidene)-5-imino-3-methyl-7-(methylthio)-5*H*-thiazolo[3,2-*a*]pyrimidine-2-carbohydrazide (5n).

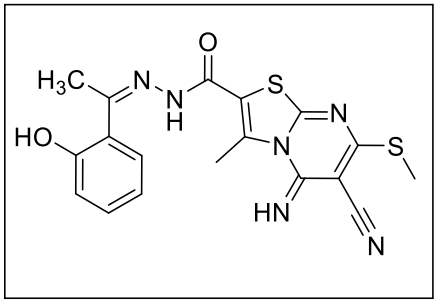

Yield 75%, mp 204–206 °C. IR spectrum, *v*, cm^{-1}: 1654.21 (C=O), 2203.66 (CN), 2926.11 (CH_3), 3283.21 (-NH). Found, %: C 52.44, H 3.88, N 20.41. $C_{18}H_{16}N_6O_2S_2$. Calculated, %: C, 52.41; H, 3.91; N, 20.37. *M* 412.

(*Z*)-6-cyano-*N*'-(1-(3-hydroxyphenyl)ethylidene)-5-imino-3-methyl-7-(methylthio)-5*H*-thiazolo[3,2-*a*]pyrimidine-2-carbohydrazide (5o).

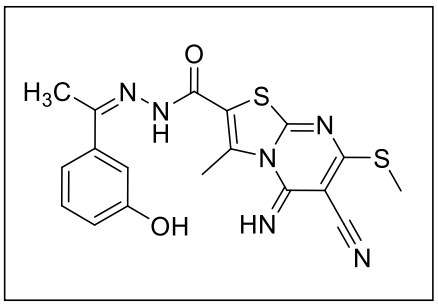

Yield 71%, mp 201–203 °C. IR spectrum, *v*, cm^{-1}: 1652.47 (C=O), 2208.84 (CN), 2933.90 (CH_3), 3277.44 (-NH). Found, %: C 52.43, H 3.89, N 20.41. $C_{18}H_{16}N_6O_2S_2$. Calculated, %: C, 52.41; H, 3.91; N, 20.37%. *M* 412.

4.4.1. Antimalarial activity of synthesized compound

The Equity Laboratory in Rajkot, Gujarat, tested all of the synthesized molecules for antimalarial activity. The in vitro antimalarial assay was conducted on 96 well microtiter plates using Rieckmann's micro assay protocol with some slight modifications [146]. RPMI 1640 medium enriched with 25 mM HEPES, 1% D-glucose, 0.23% sodium bicarbonate, and heat-inactivated 10% human serum was used to preserve the cultures of Plasmodium Falciparum 3D7 strain. The ring stage parasitized cells were obtained by synchronizing the asynchronous parasites of Plasmodium falciparum with 5% D-sorbitol treatment[147]. The experiment required a sample with a parasitaemia of 0.8 to 1.5% at a 3% hematocrit level in a 200 µl medium of RPMI-1640. Using JSB staining, the sample was evaluated to determine its parasitaemia percentage and kept with 50% RBCs (O+)[148] DMSO was used to prepare a stock solution containing 5mg/ml of each test sample, followed by dilutions with culture medium. Duplicate wells, containing parasitized cell preparation, were loaded with diluted samples at a volume of 20 µl resulting in final concentrations (at five-fold dilutions) ranging from 0.4 µg/ml to 100 µg/ml[149]. A candle jar was utilized to incubate the culture plates at 37 °C. Thin blood smears were created from each well after an incubation period of 36 to 40 hours and then subjected to JSB staining[150]. The process of ring stage parasites transitioning into trophozoites and schizonts was carefully monitored through the use of varying concentrations of the test agents under microscopic observation. The test found the minimum inhibitory concentrations (MIC) that stopped the complete maturation into schizonts[151]. Chloroquine was used as the reference drug. After 38 hours of incubation, the average of the trophozoites, number of rings and schizonts per 100 parasites was determined, and the percent inhibition of maturation relative to control group was determined.

4.4.2. Experimental protocol of molecular docking study

The ChemSketch 2022.2.3. was utilized for the design of ligand structures. Additionally, the docking investigations were also performed using the Autodock Vina 1.5.7 platform[99]. The PDB database provided the crystallographic data for the PfDHFR enzyme with PDB id 3QGT. The energy minimization of the ligands was meticulously performed using Avogadro software, employing the MMFF94 force field to ensure precise optimization of their molecular structures, thereby enhancing the accuracy and reliability of our computational studies. Heteroatoms were excluded to ensure that the structural receptor was devoid of any ligand before docking. To prepare the protein, polar hydrogens and kollaman charge were introduced, while water was eliminated. The grid box dimensions for x, y, and z were configured to be 20 Å each, and their respective centers were established at 28.034765, 5.436353, and 58.756000. The spacing among grid points was 0.375 angstroms and the exhaustiveness was set at a value of 8. Discovery studio v21.1.0.20298 was utilized to finding the probable binding mode[152].

4.5. Spectral Data

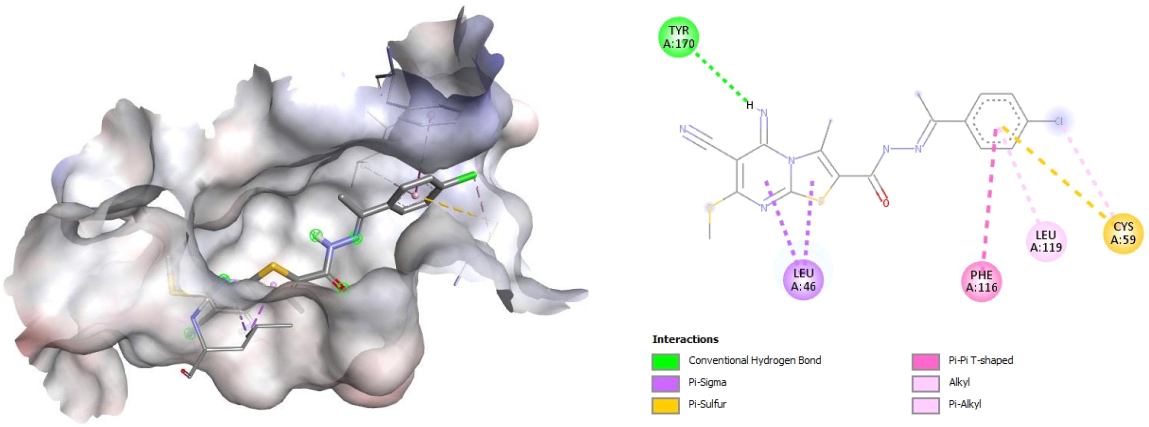

Fig. 1: Representative 2D & 3D molecular docking data of compound **JTAM-2**

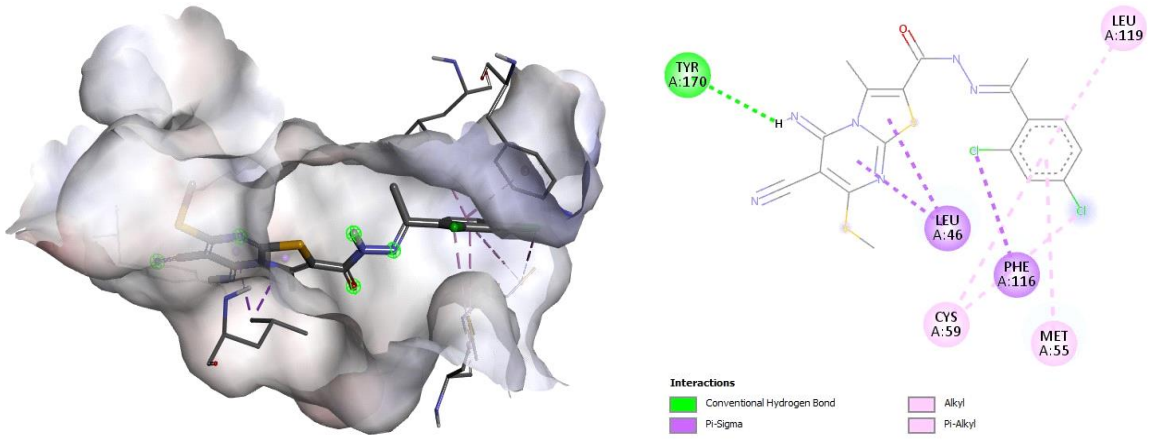

Fig. 2: Representative 2D & 3D molecular docking data of compound **JTAM-6**

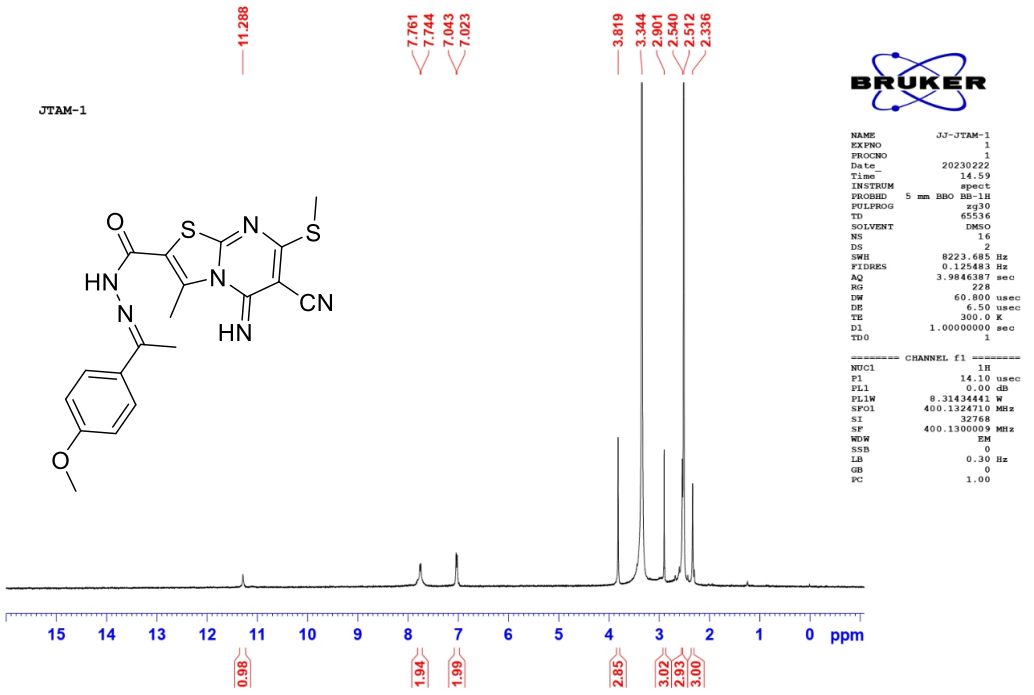

Fig. 3: Representative ^{1}H NMR spectrum of compound **JTAM-1**

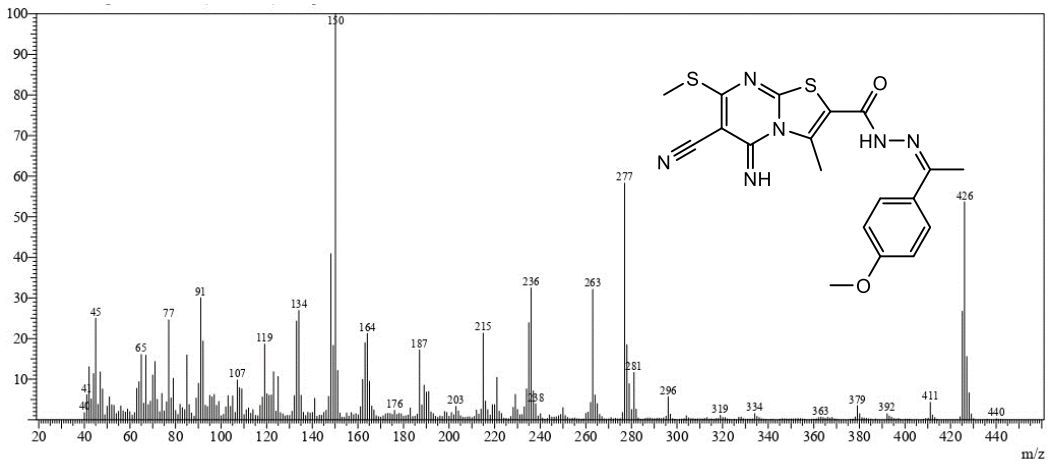

Fig. 4: Representative mass spectrum of compound **JTAM-1**

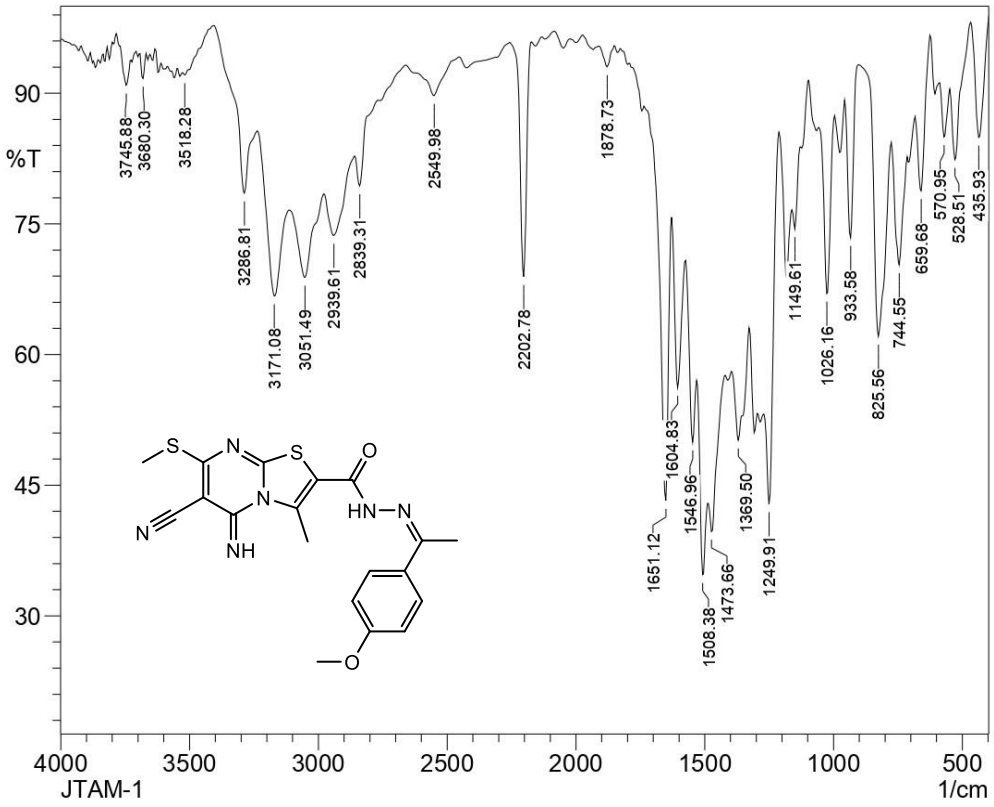

Fig. 5: Representative IR spectrum of compound **JTAM-1**

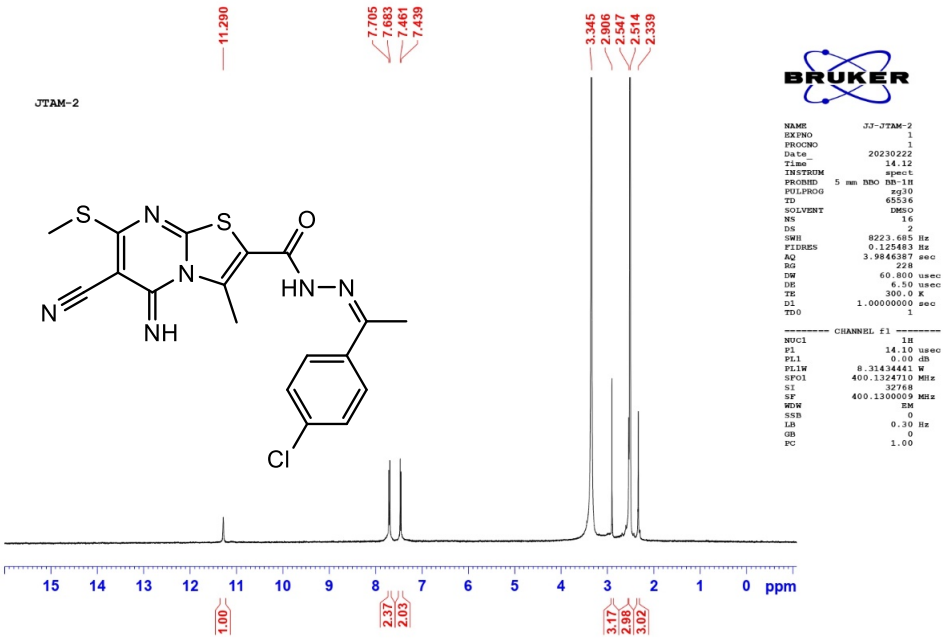

Fig. 6: Representative ^{1}H NMR spectrum of compound **JTAM-2**

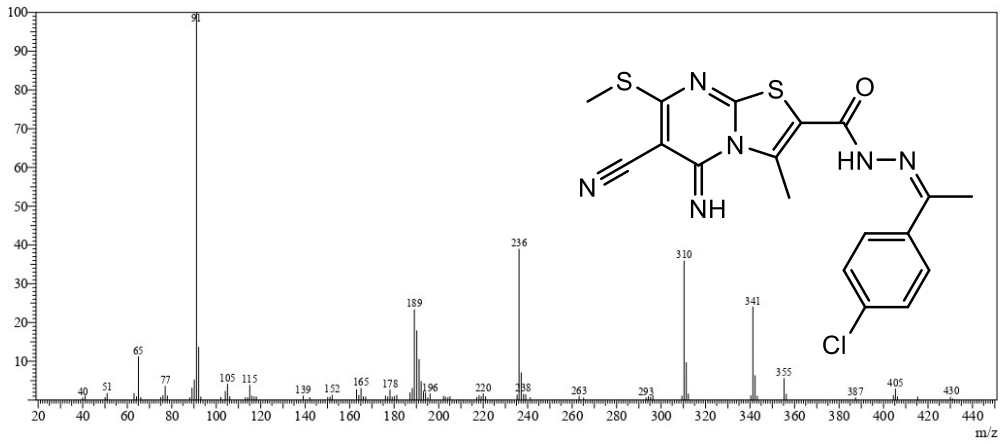

Fig. 7: Representative mass spectrum of compound **JTAM-2**

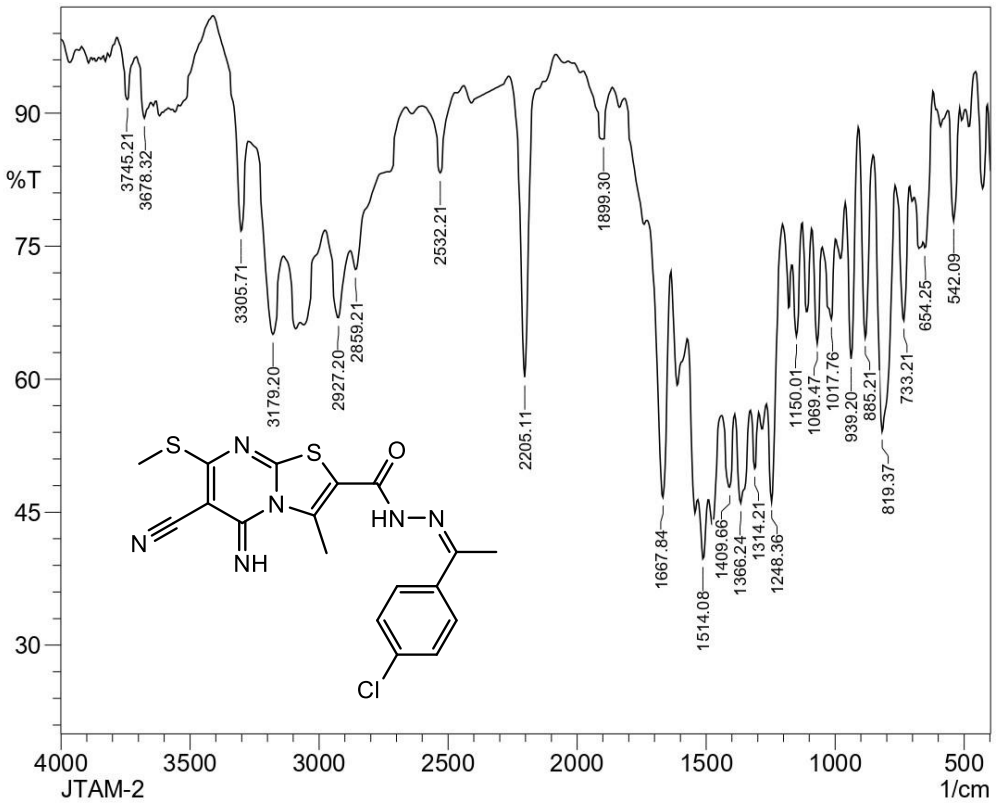

Fig. 8: Representative IR spectrum of compound **JTAM-2**

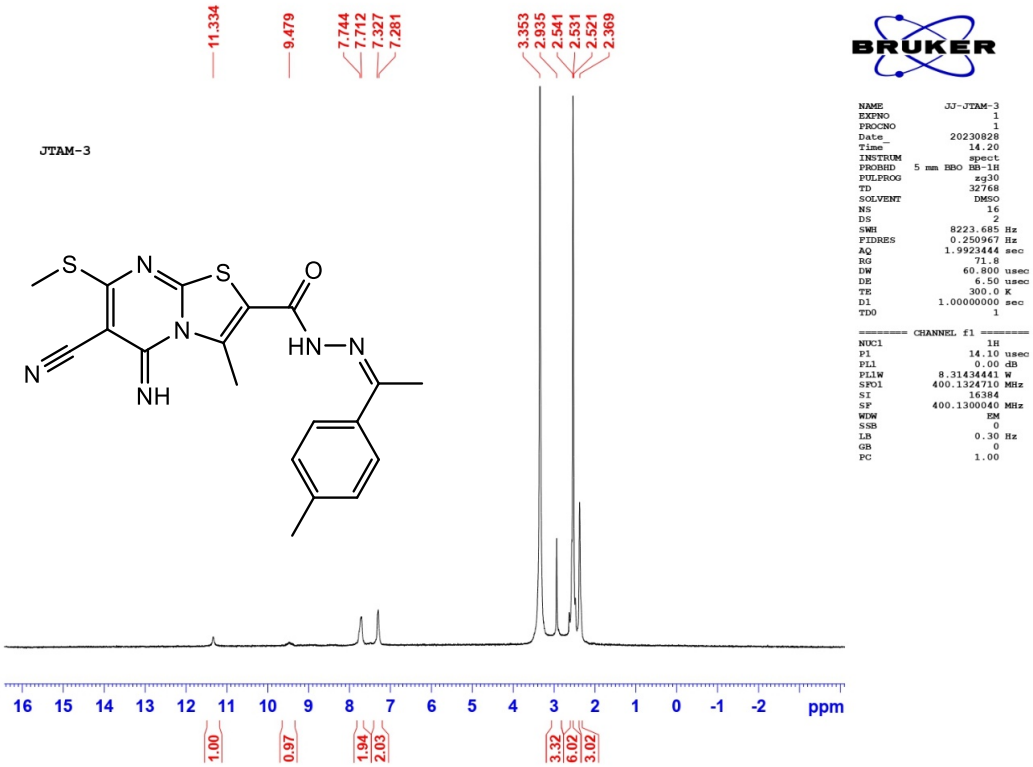

Fig. 9: Representative ^{1}H NMR spectrum of compound **JTAM-3**

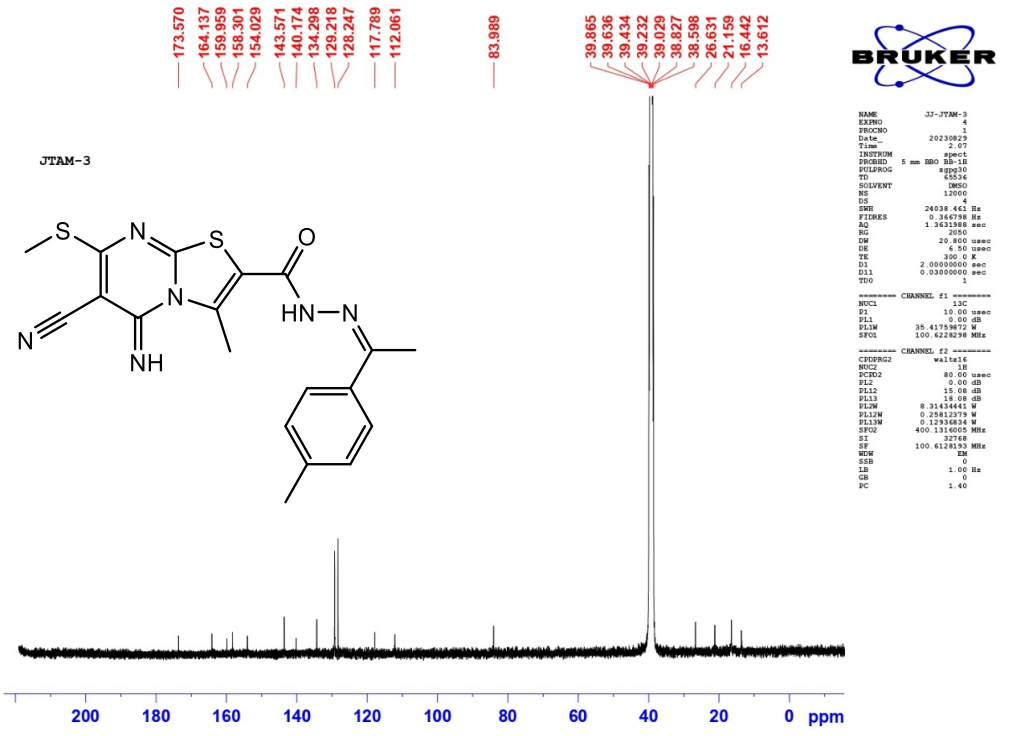

Fig. 10: Representative ^{13}C NMR spectrum of compound **JTAM-3**

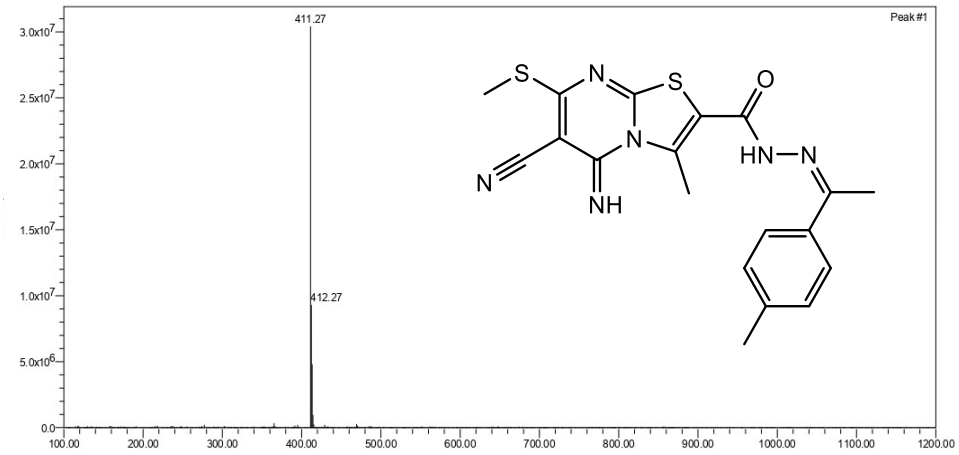

Fig. 11: Representative mass spectrum of compound **JTAM-3**

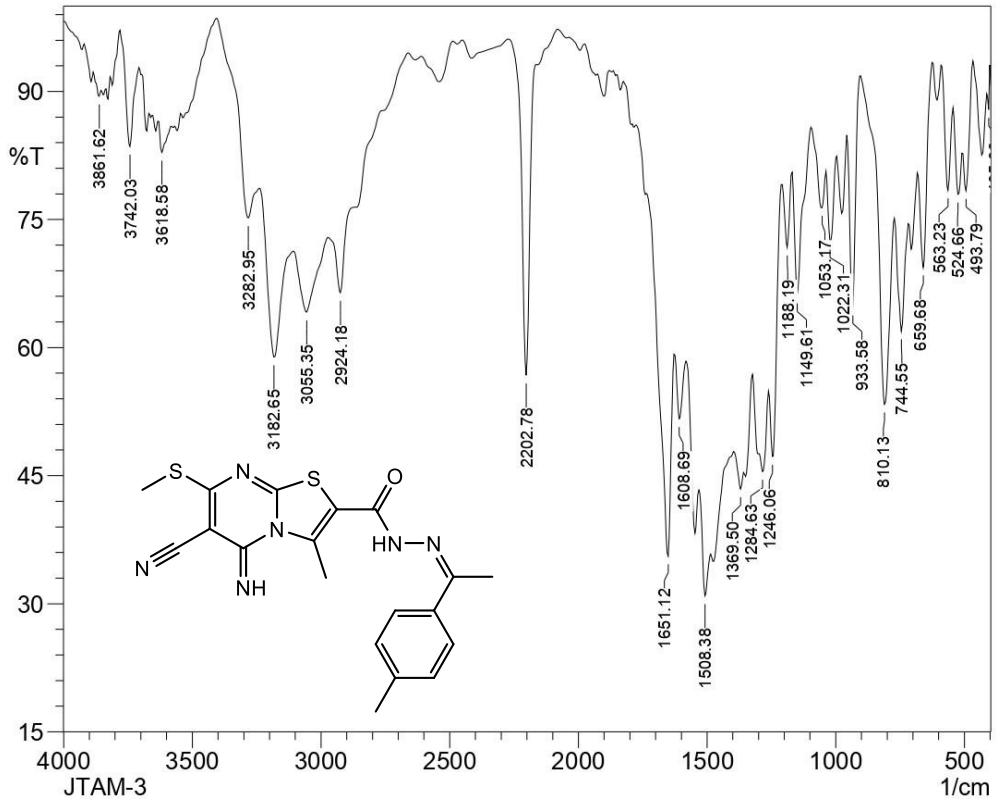

Fig. 12: Representative IR spectrum of compound **JTAM-3**

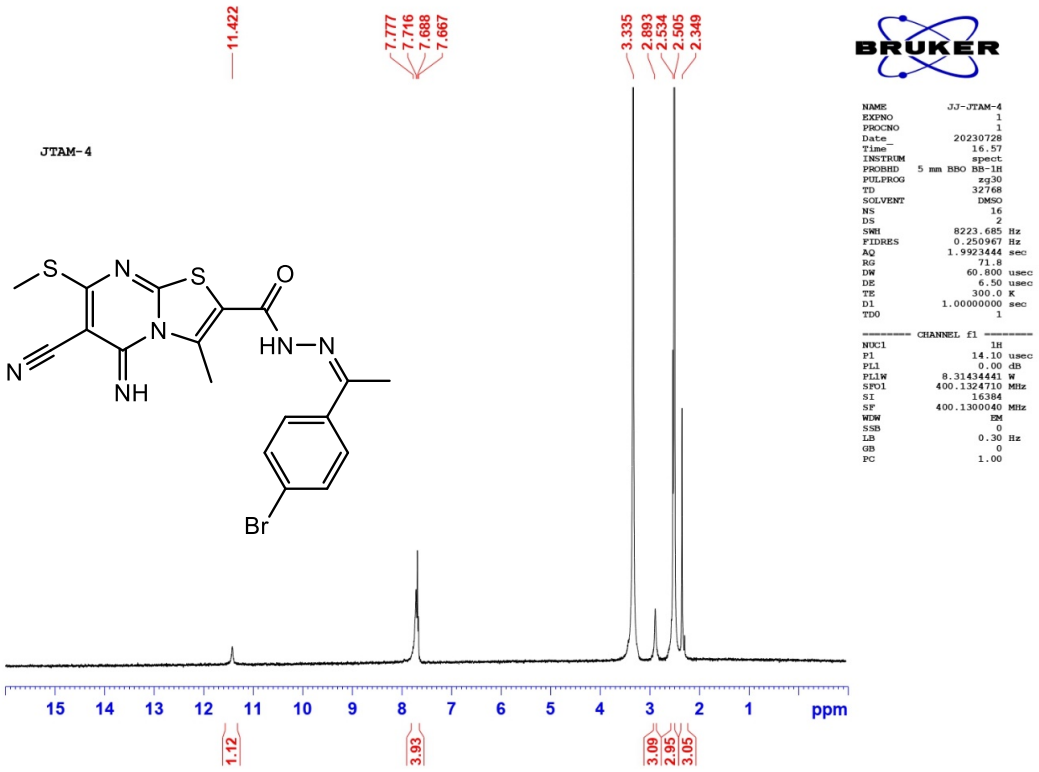

Fig. 13: Representative ^{1}H NMR spectrum of compound **JTAM-4**

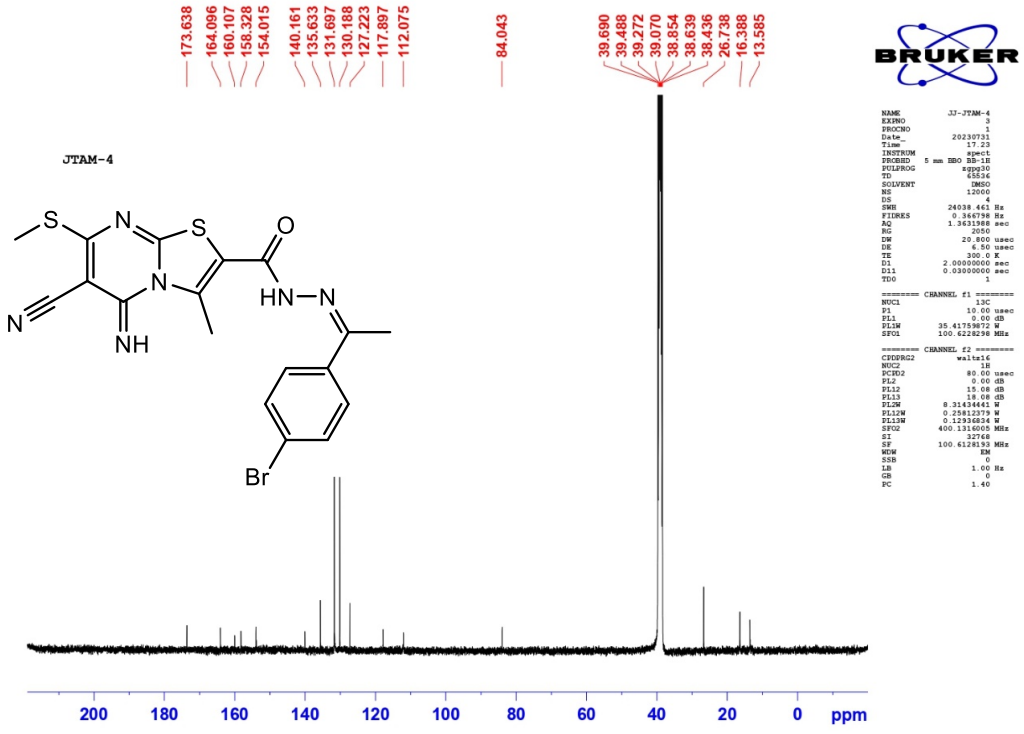

Fig. 14: Representative ^{13}C NMR spectrum of compound **JTAM-4**

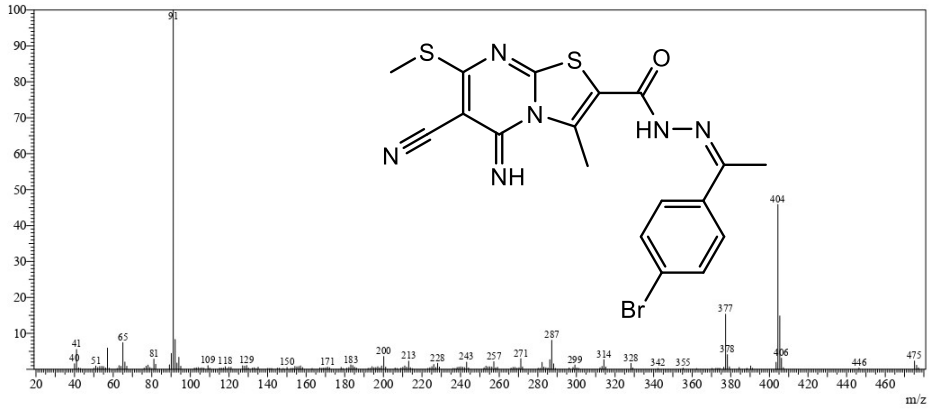

Fig. 15: Representative mass spectrum of compound **JTAM-4**

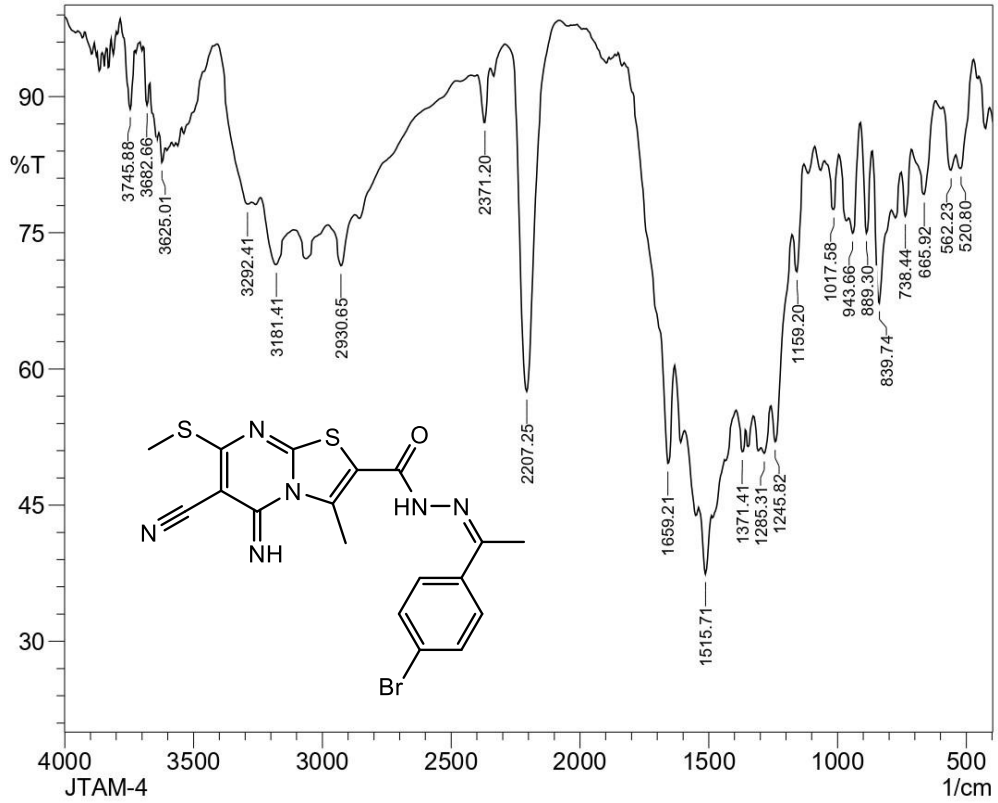

Fig. 16: Representative IR spectrum of compound **JTAM-4**

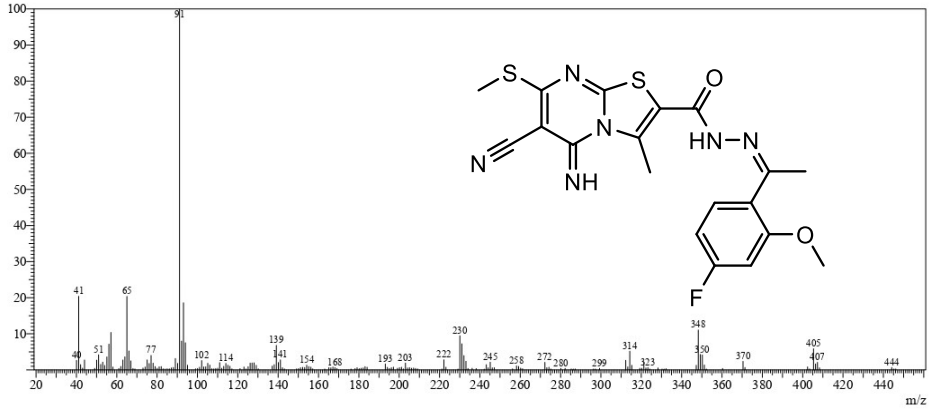

Fig. 17: Representative mass spectrum of compound **JTAM-5**

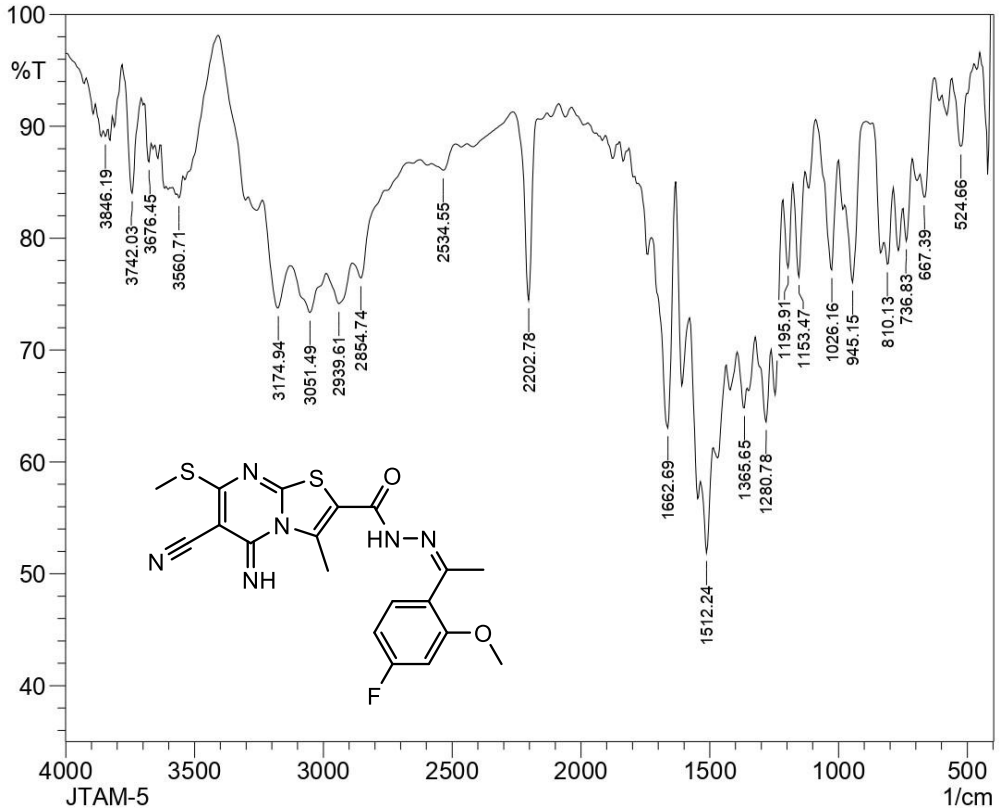

Fig. 18: Representative IR spectrum of compound **JTAM-5**

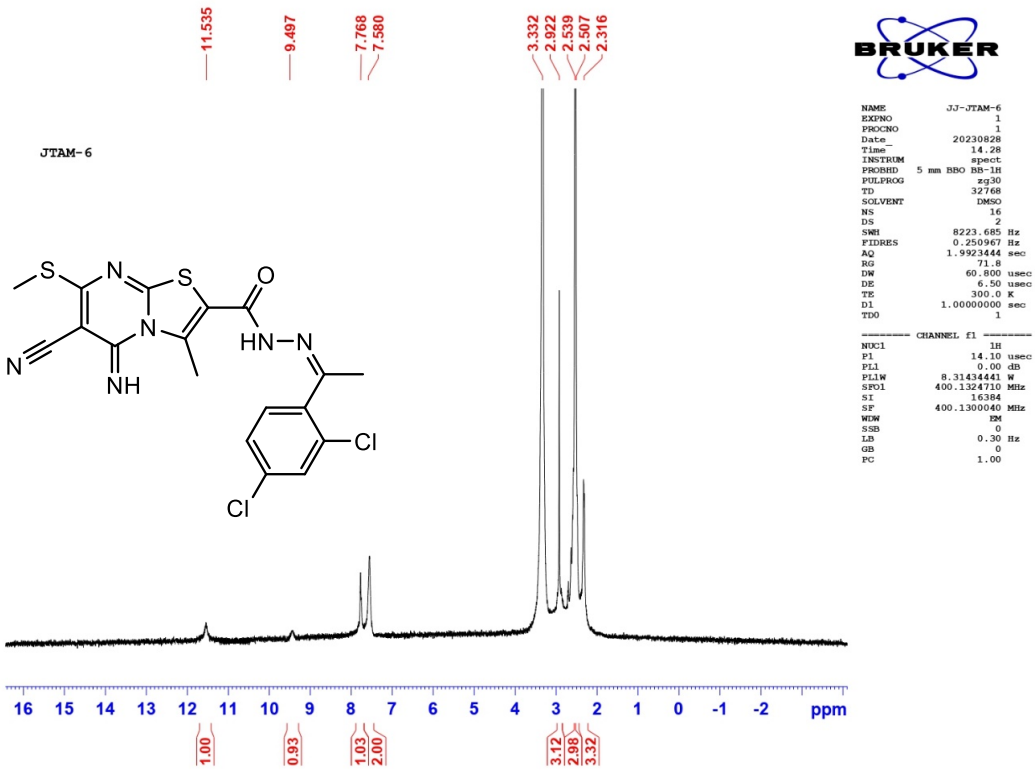

Fig. 19: Representative ^{1}H NMR spectrum of compound **JTAM-6**

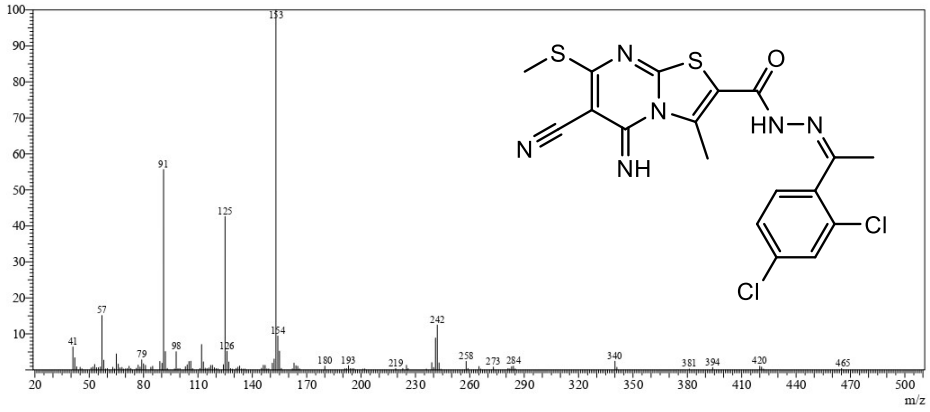

Fig. 20: Representative mass spectrum of compound **JTAM-6**

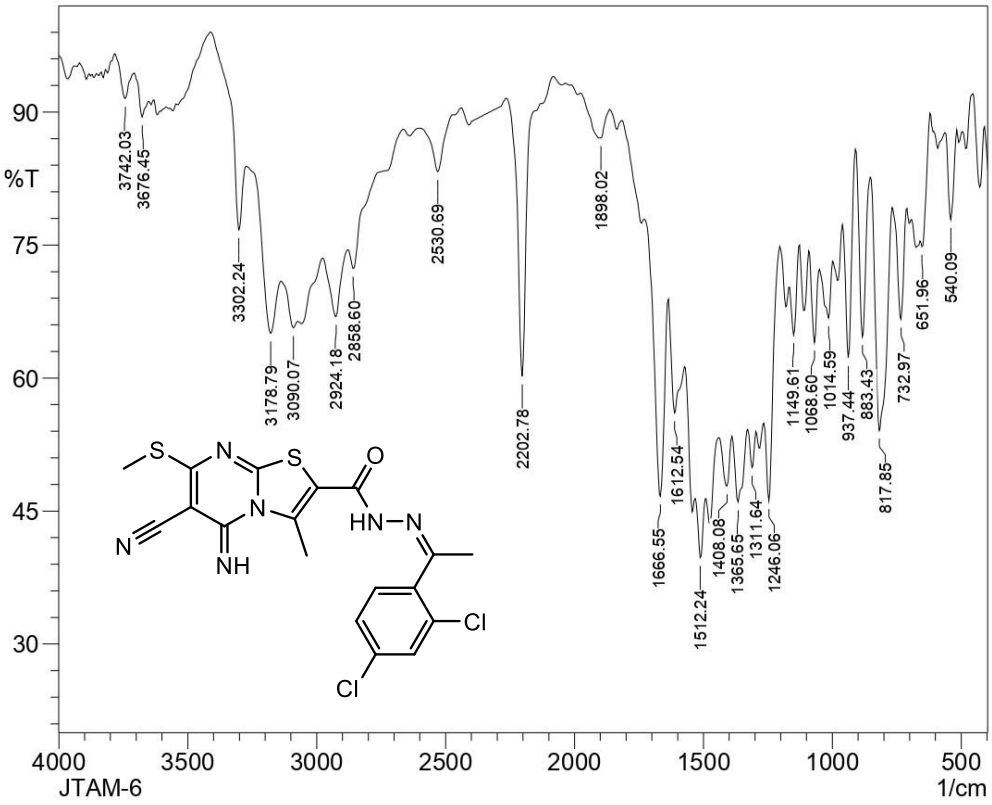

Fig. 21: Representative IR spectrum of compound **JTAM-6**

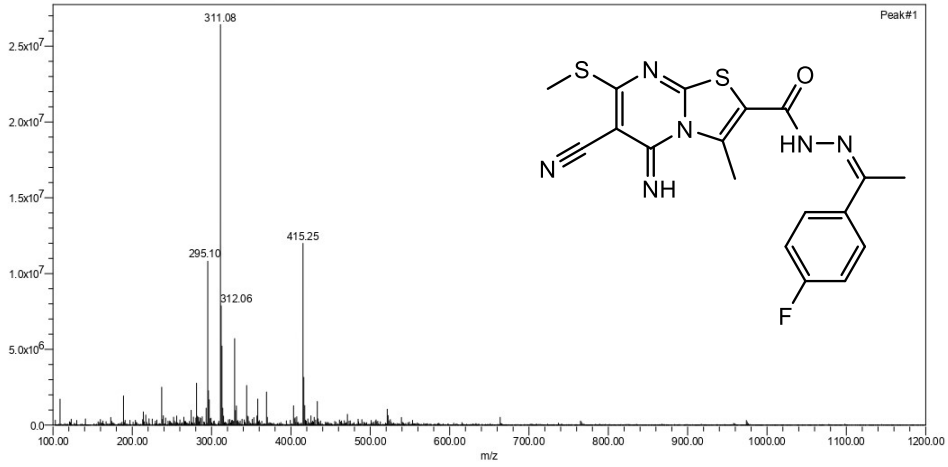

Fig. 22: Representative mass spectrum of compound **JTAM-7**

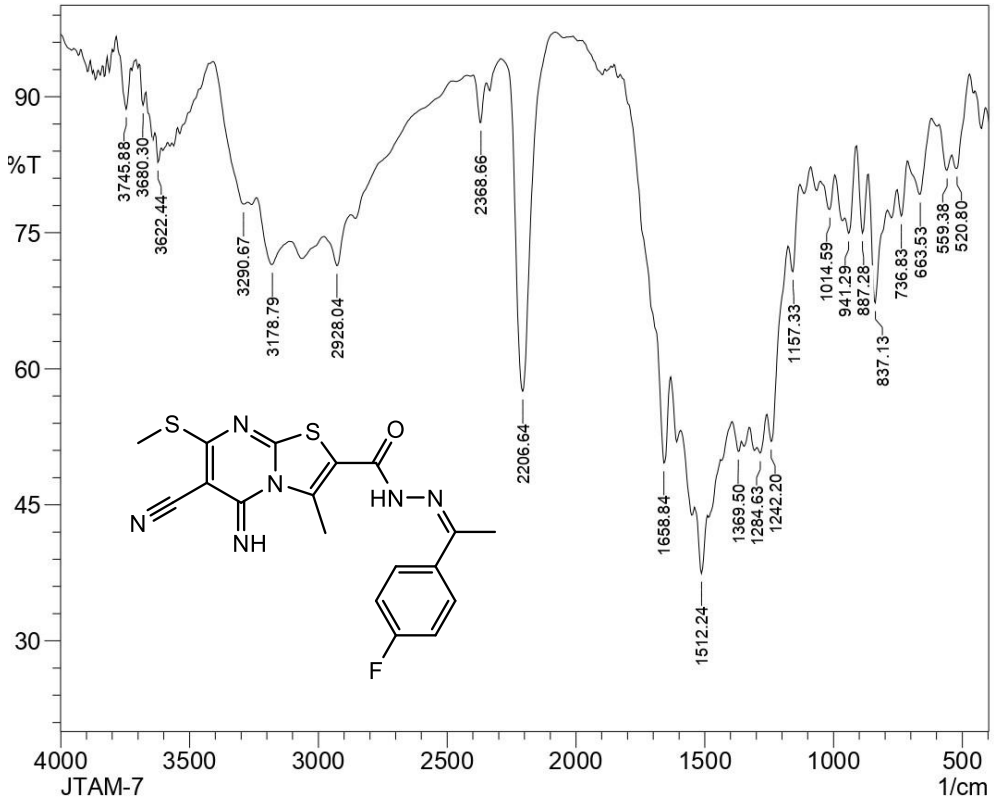

Fig. 23: Representative IR spectrum of compound **JTAM-7**

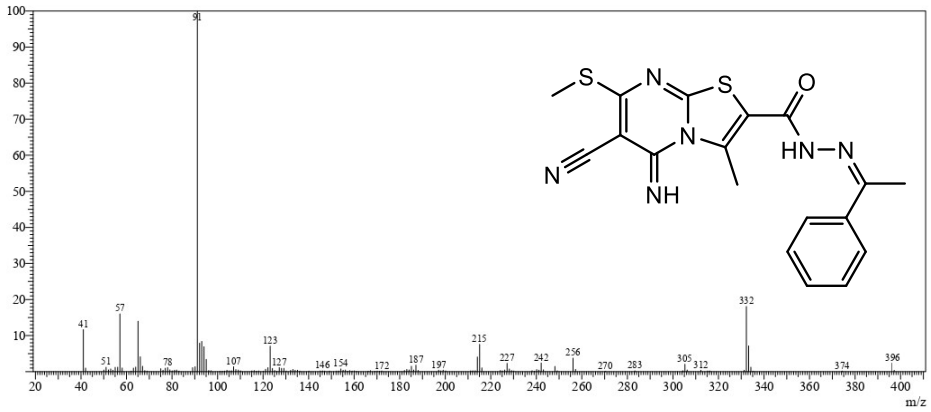

Fig. 24: Representative mass spectrum of compound **JTAM-8**

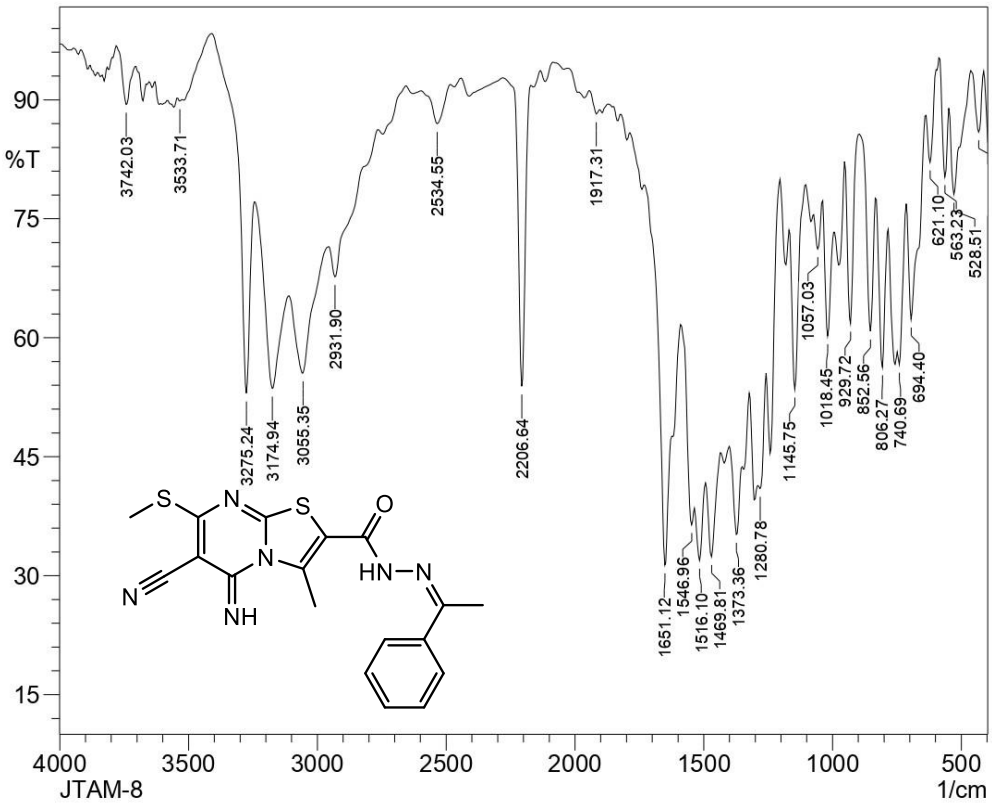

Fig. 25: Representative IR spectrum of compound **JTAM -8**

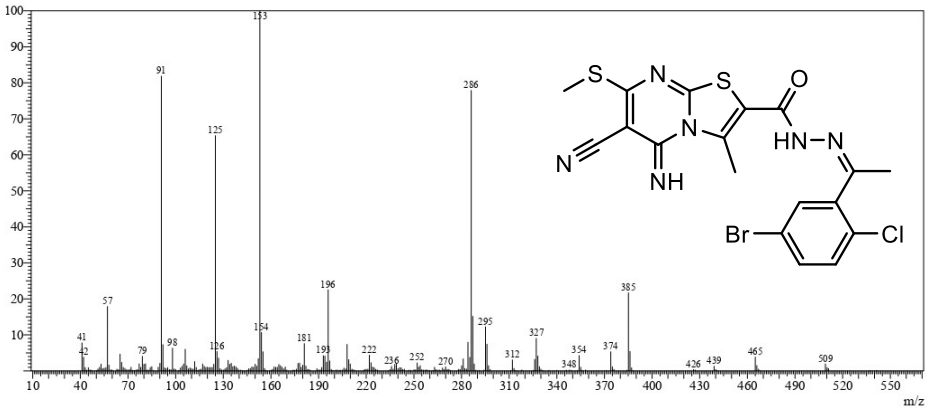

Fig. 26: Representative mass spectrum of compound **JTAM-9**

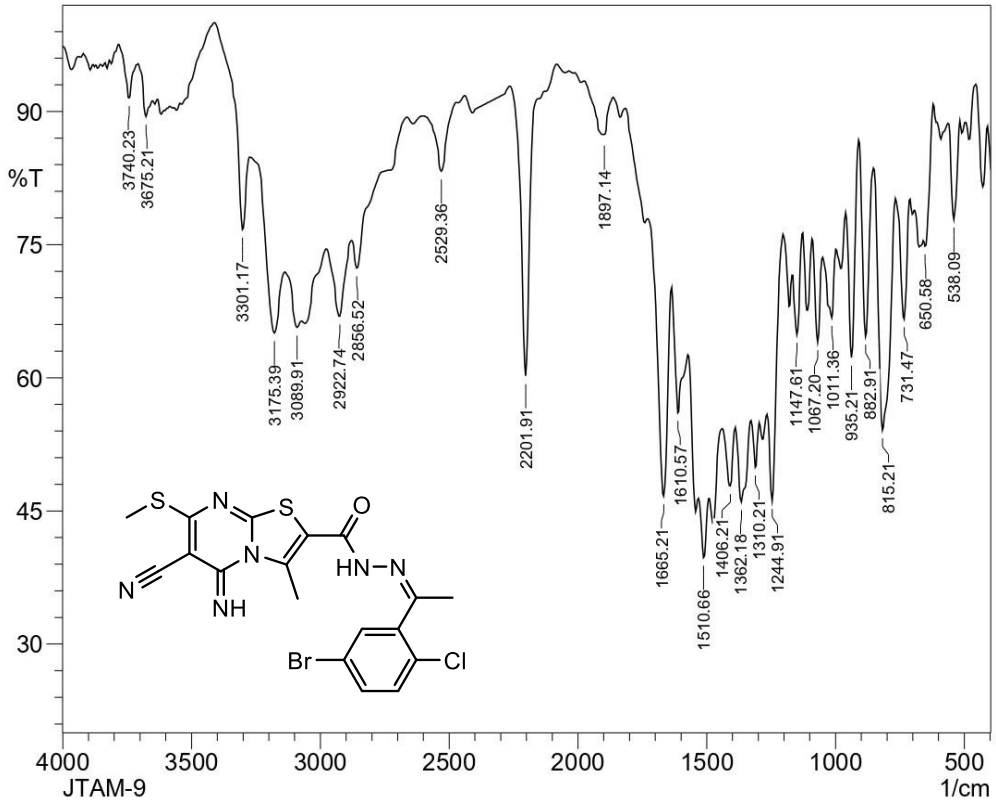

Fig. 27: Representative IR spectrum of compound **JTAM -9**

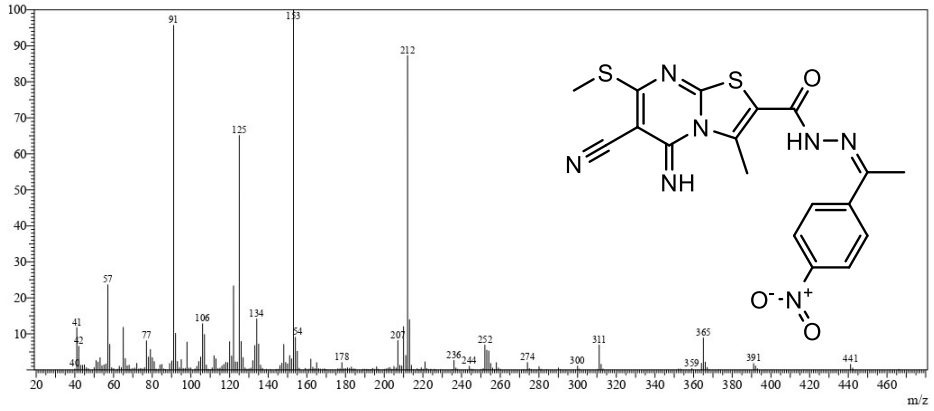

Fig. 28: Representative mass spectrum of compound **JTAM-10**

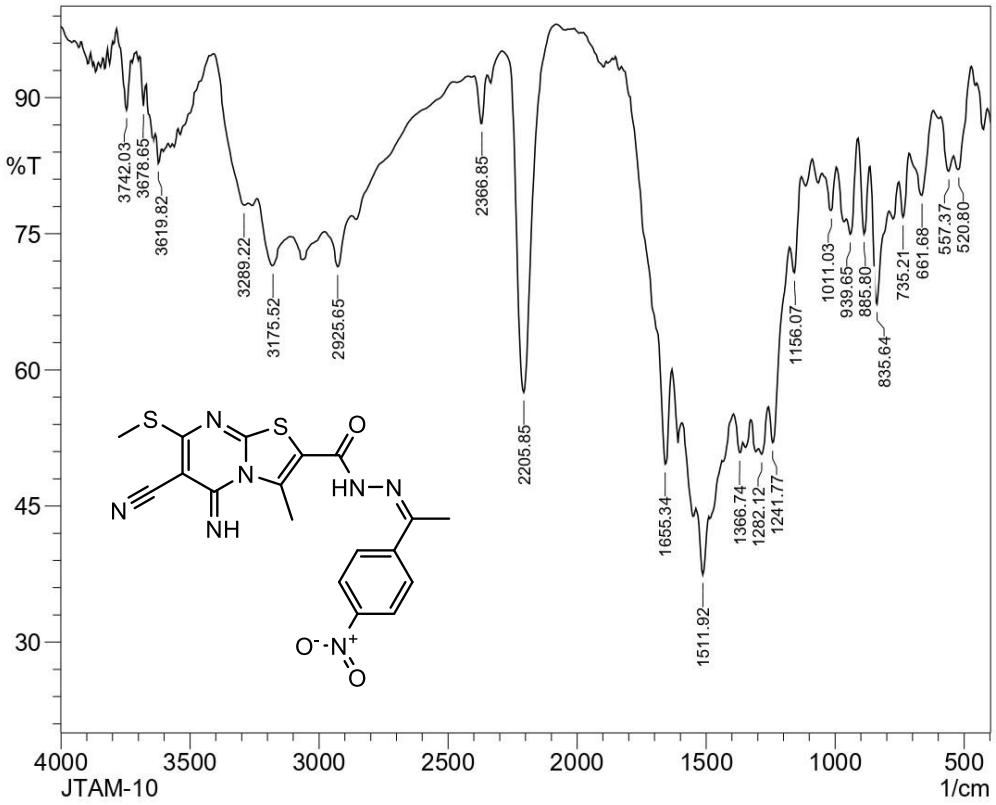

Fig. 29: Representative IR spectrum of compound **JTAM -10**

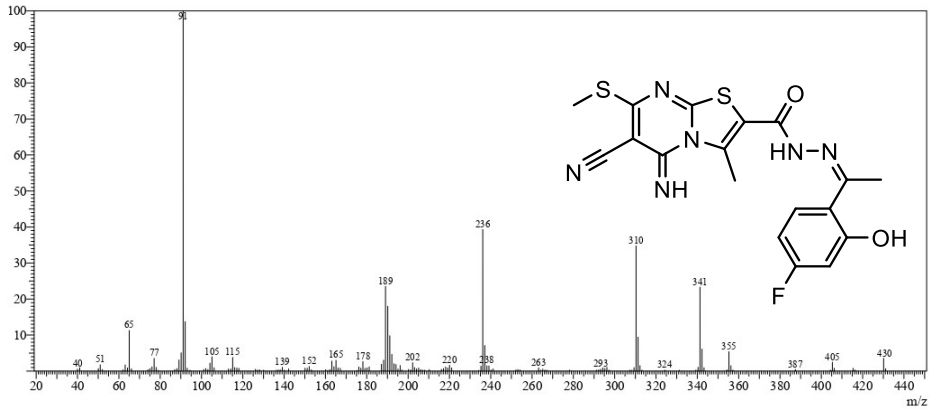

Fig. 30: Representative mass spectrum of compound **JTAM-11**

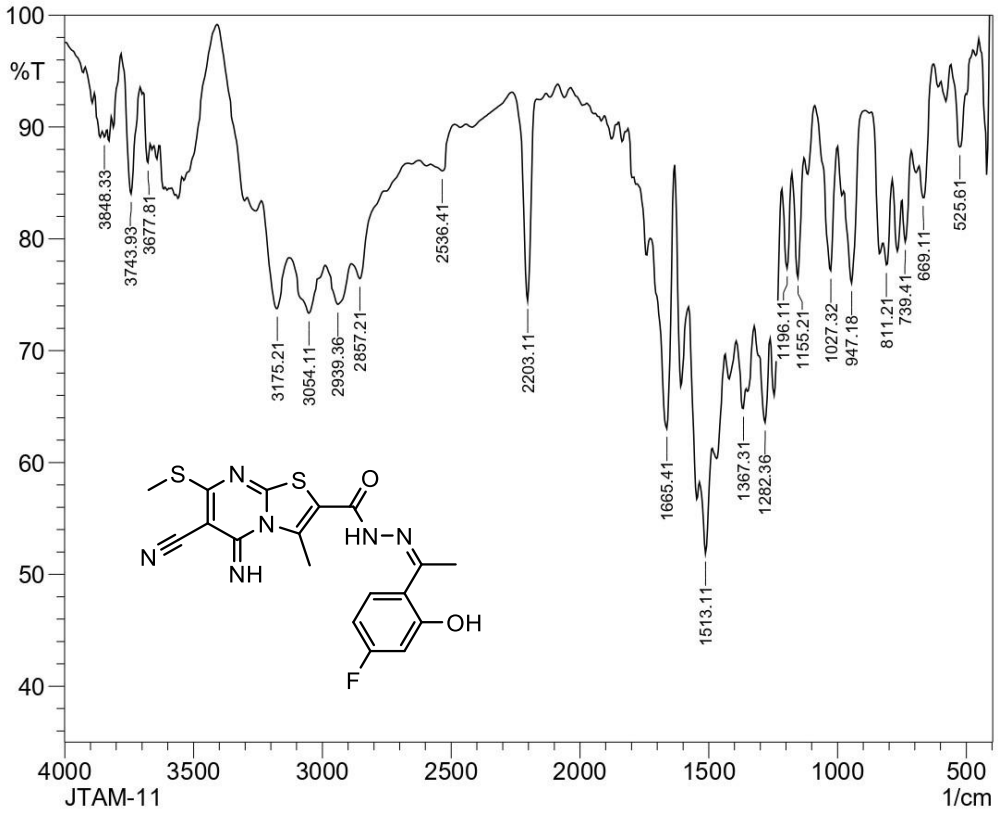

Fig. 31: Representative IR spectrum of compound **JTAM -11**

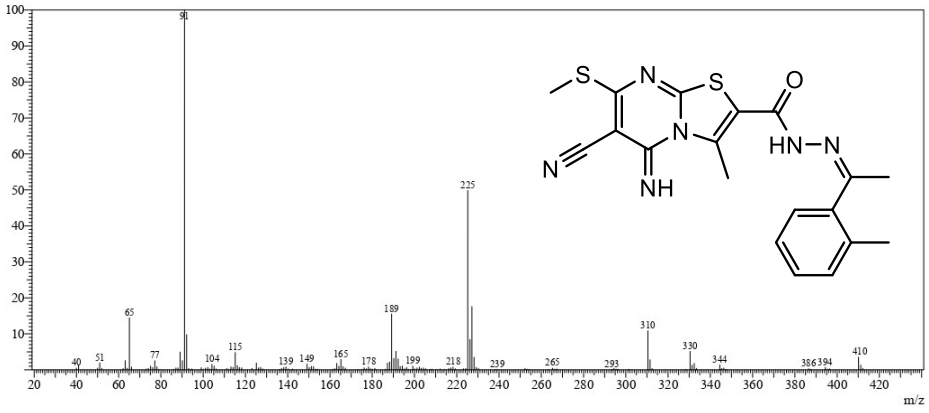

Fig. 32: Representative mass spectrum of compound **JTAM-12**

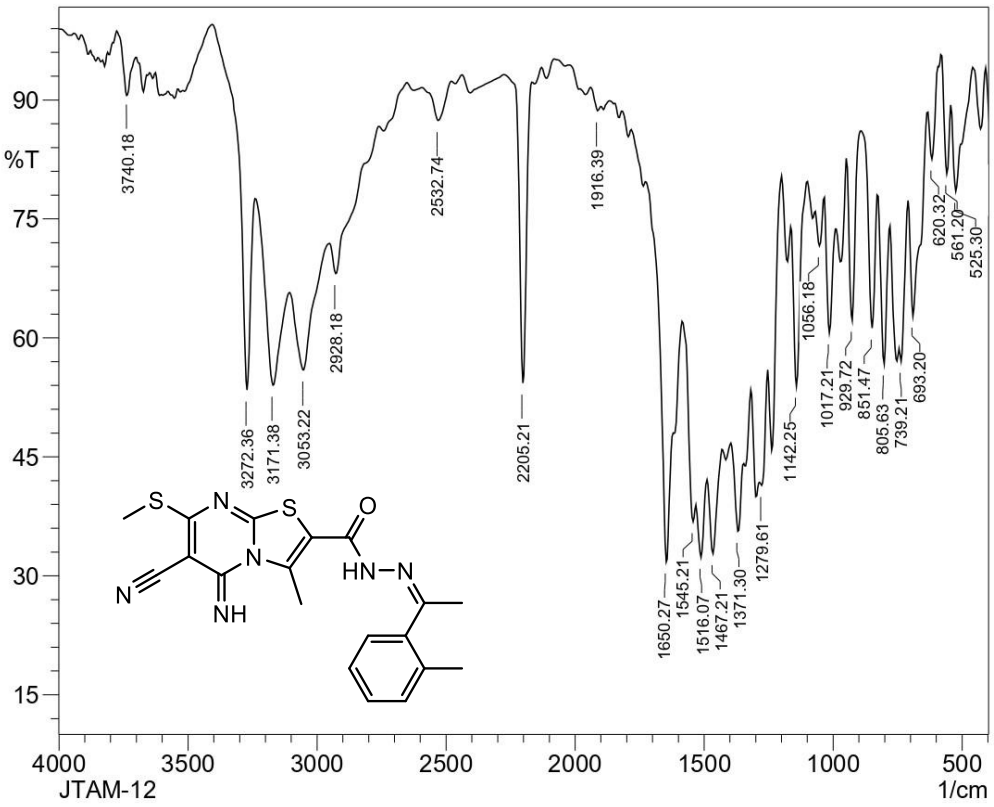

Fig. 33: Representative IR spectrum of compound **JTAM-12**

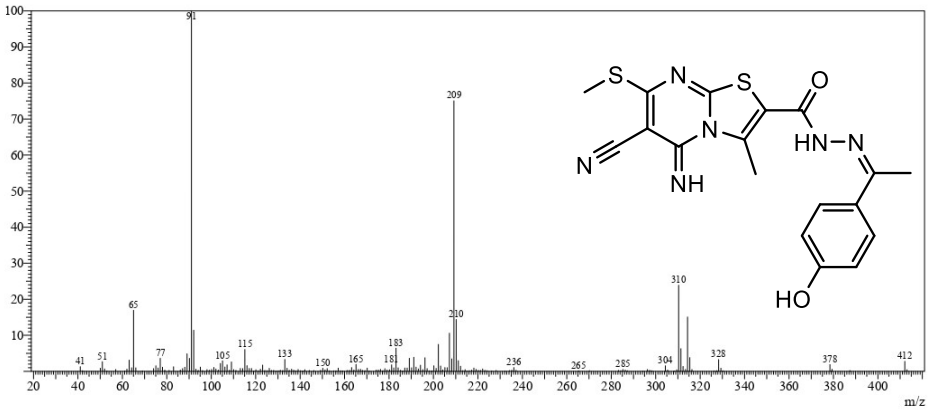

Fig. 34: Representative mass spectrum of compound **JTAM-13**

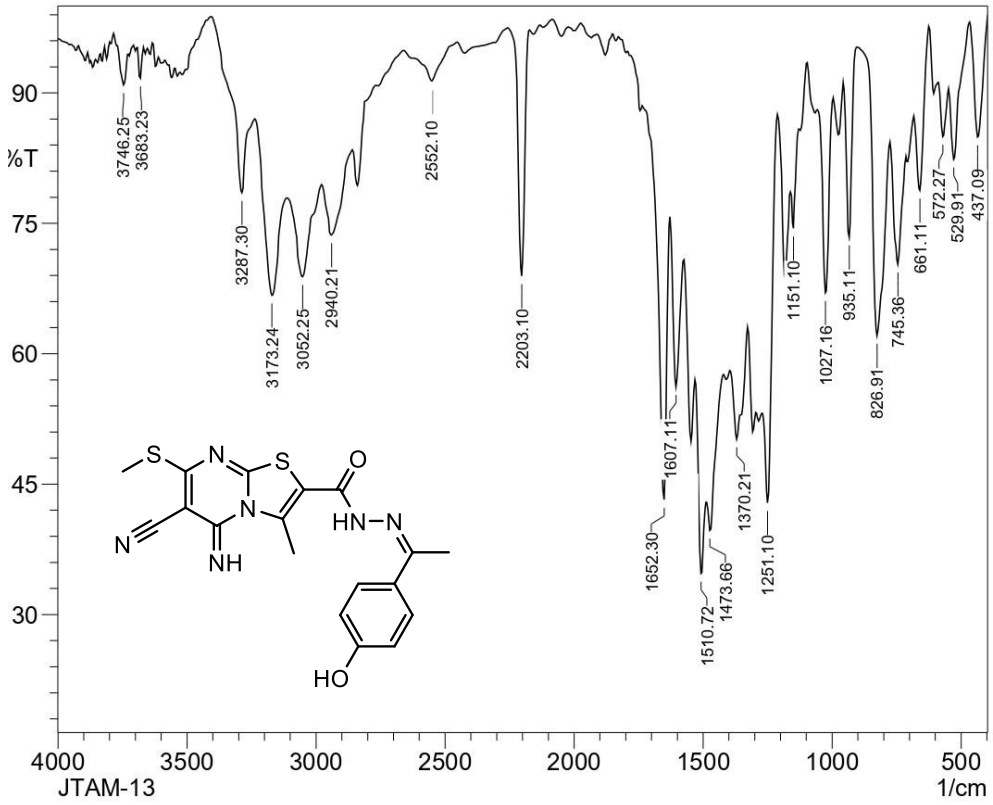

Fig. 35: Representative IR spectrum of compound **JTAM -13**

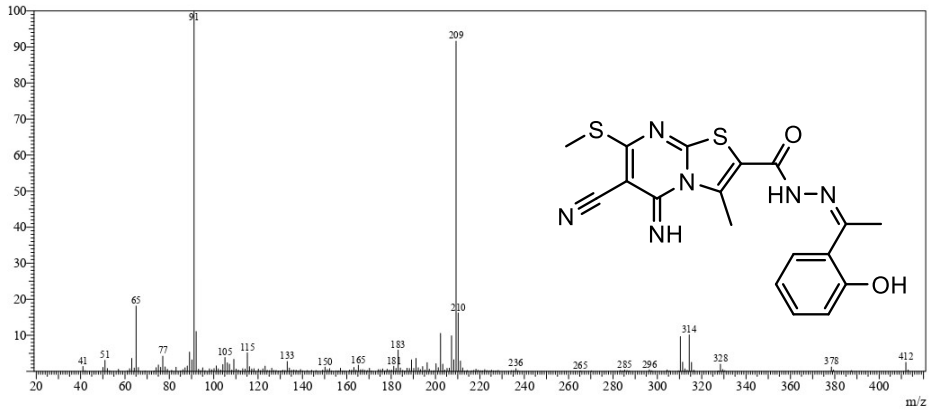

Fig. 36: Representative mass spectrum of compound **JTAM-14**

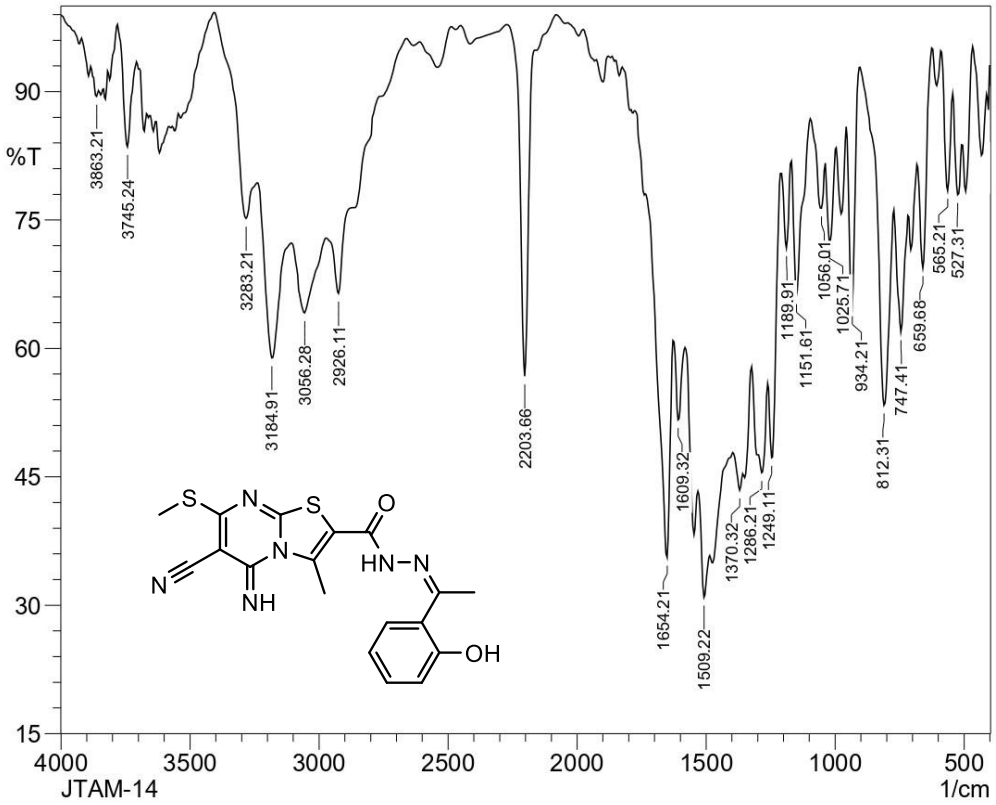

Fig. 37: Representative IR spectrum of compound **JTAM -14**

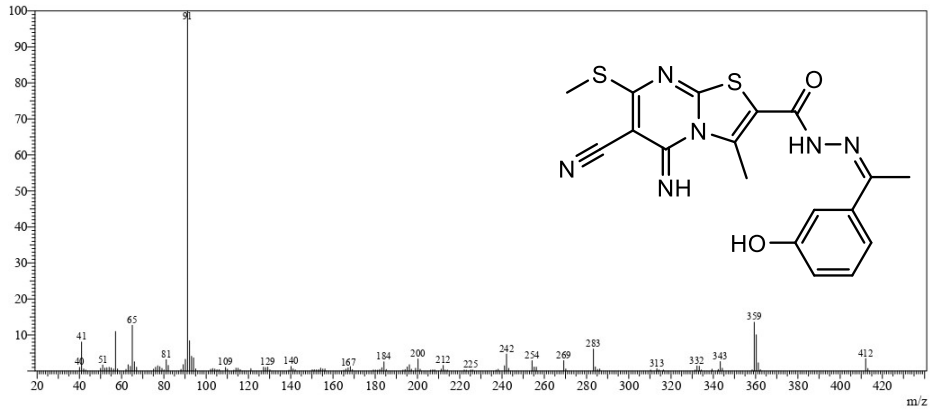

Fig. 38: Representative mass spectrum of compound **JTAM-15**

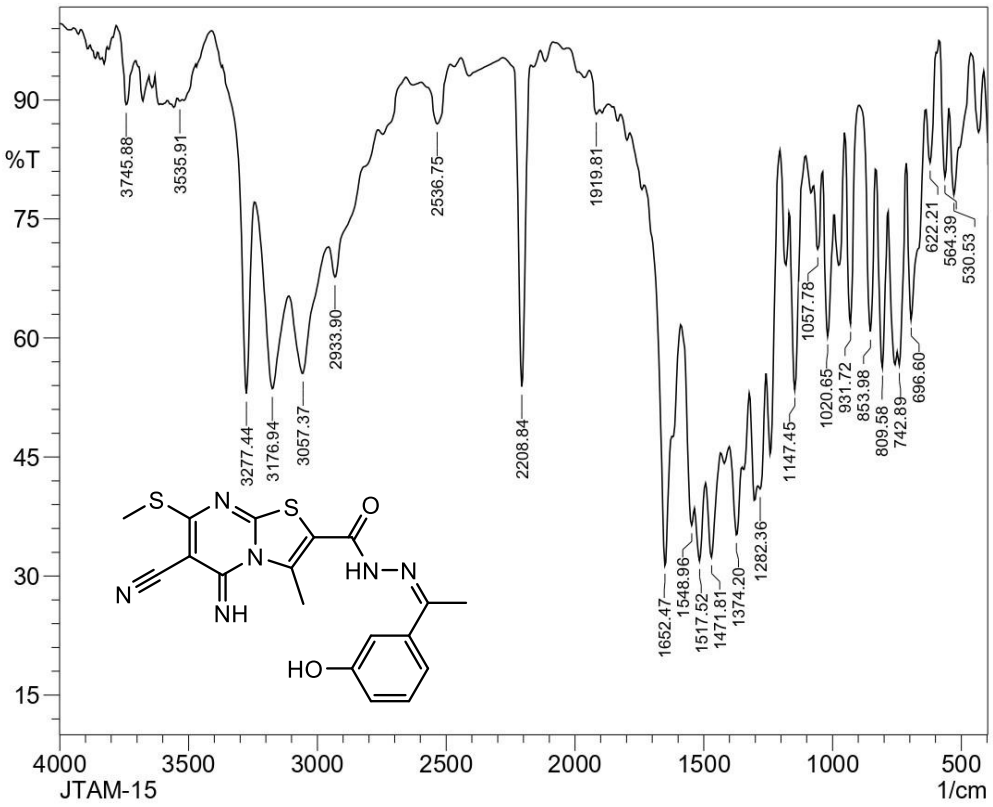

Fig. 39: Representative IR spectrum of compound **JTAM -15**